

6-7-2010

Use of Inorganic Quantum Dot-Cationic Liposome Hybrids for the Delivery and Expression of Calcium-Sequestering Parvalbumin into Mammalian Cell Cultures

Charles Christian Ellis
Florida State University

Follow this and additional works at: <http://diginole.lib.fsu.edu/etd>

Recommended Citation

Ellis, Charles Christian, "Use of Inorganic Quantum Dot-Cationic Liposome Hybrids for the Delivery and Expression of Calcium-Sequestering Parvalbumin into Mammalian Cell Cultures" (2010). *Electronic Theses, Treatises and Dissertations*. Paper 571.

This Thesis - Open Access is brought to you for free and open access by the The Graduate School at DigiNole Commons. It has been accepted for inclusion in Electronic Theses, Treatises and Dissertations by an authorized administrator of DigiNole Commons. For more information, please contact lib-ir@fsu.edu.

THE FLORIDA STATE UNIVERSITY
COLLEGE OF ARTS AND SCIENCES

USE OF INORGANIC QUANTUM DOT-CATIONIC LIPOSOME HYBRIDS
FOR THE DELIVERY AND EXPRESSION OF CALCIUM-SEQUESTERING
PARVALBUMIN INTO MAMMALIAN CELL CULTURES

By

CHARLES CHRISTIAN ELLIS

A Thesis Submitted to the
Department of Chemistry and Biochemistry
in partial fulfillment of the
requirements for the degree of
Master of Science

Degree Awarded:
Summer Semester, 2010

The members of the committee approve the thesis of Charles Ellis defended on June 7th, 2010:

Geoffrey Strouse
Professor Directing Thesis

Timothy Logan
Committee Member

Hong Li
Committee Member

The Graduate School has verified and approved the above-named committee members.

ACKNOWLEDGEMENTS

I would like to thank my Adviser and Principal Investigator Dr. Geoffrey Strouse for giving me the opportunity, support and intellectual freedom to complete this degree as well as our collaborating investigator Dr. Timothy Logan for support, both financial, personal and intellectual. I would like to thank all the members of the Strouse and Logan labs who have helped me and been my friends during my time here: Chris Ridel, Chris Breshike, Megan Muroski, Nathalie Munoz, Abigail Goodyear, David Skelton, Lawrence Walker, Brian Stapleton, Kyle Noble, Steven Hira, Dr. Derek Lovingood, Dr. Josh Kogot and Dr. Steven Yun.

I also give thanks to Dr. Scott Stagg and Dr. Jason O'Donnell for their work in Cryo-Electron Microscopy. I'd like to thank Dr. Claudius Mundoma for his help with a number of instruments and techniques over the years. I owe thanks to Dr. Joan Hare, who in addition to training me in mammalian cell culture technique has been a consistently benevolent presence in my research experience here at FSU. I'd like to thank Dr. Ruth Didier for her help with flow cytometry experiments.

I'd like to thank Dr. Brenda Schoffstall of Barry University for training me in cardiomyocyte isolation, Dr. Jeffrey Robbins of University of Cincinnati for his donation of plasmids for my research, the FSU Sequencing Facility for all their work, Dr. Moerland for donation of the Parvalbumin gene and lab member Carl Wittington for consultation, advice and being a friend.

I'd like to thank Dr. Kerry Maddox for all of her help over the last few years and being someone who genuinely cared about the students. Also, I'd like to thank all the students, administrators, specialists, officers and maintenance of the Molecular Biophysics department who have made the last three years memorable and pleasant.

I'd like to thank my family and friends for all the support and for making life worth living. Life has little meaning or purpose without your love and favor.

Finally I would like to thank Dr. Hong Li. You have done more for me in the last 5 years than I could have expected from anyone. Whatever I needed, Dr. Li has given without hesitation. Whether you know it or not, your influence changed my life forever in the best way possible. Thank you so much for everything. God bless you.

TABLE OF CONTENTS

List of Figures.....	v
List of Abbreviations.....	vii
Abstract.....	viii
Introduction.....	1
Role of Parvalbumin in Correcting Diastolic Dysfunction.....	1
Gene Therapy Techniques and Integration of Nanomaterials.....	4
Aims of Study.....	8
Materials and Methods.....	9
Cloning of Parvalbumin onto N-terminus of mCherry(CMV).....	9
Site-Directed Mutagenesis to Remove Internal Kozak Sequence.....	13
Sub-Cloning of PV-mCherry into α -MyHC Promoter.....	16
Preparation of CdSe/ZnS Quantum Dots.....	20
Encapsulation of CdSe/ZnS into Cationic Liposomes.....	23
Cell Culture and Transfection Experiments.....	25
Western Blot Analysis.....	26
Dynamic Light Scattering.....	31
Wide Field Fluorescence Microscopy.....	31
Cryo-Electron Microscopy.....	32
Flow Cytometry.....	33
Results and Discussion.....	34
Cloning and Expression of PV-mCherry Fusion Protein.....	34
Synthesis of CdSe/ZnS and Encapsulation into Liposomes.....	46
Internalization of LQD, Association and Delivery of DNA into CHO cells.....	49
Conclusions and Future Directions of Research.....	60
References.....	62
Biographical Sketch.....	64

LIST OF FIGURES

<u>1.1-</u> Effect of Parvalbumin on the Contractility Rates of Diseased Rat Cardiomyocytes.....	2
<u>1.2-</u> Effect of Lipid:DNA Mixing Ratios on the Transfection Rates in Various Cell Lines.....	5
<u>2.1a -</u> 5' PCR forward primer for the production of PV-mCherry fusion protein.....	10
<u>2.1b -</u> 3' PCR reverse primer for the production of PV-mCherry fusion protein.....	11
<u>2.2 -</u> Primers used for SDM of PV-mCherry Fusion to remove internal Kozak sequence...	15
<u>2.3 -</u> Primers used to remove Hind III cut site in Parvalbumin Gene via SDM.....	17
<u>2.4 -</u> Reverse primer for PCR PV-mCherry subcloning into α -MyHC.....	18
<u>2.5 -</u> Typical arrangement of 3-Neck Flask synthesis vessel used for ZnS shelling.....	23
<u>3.1 -</u> Agarose Gel of PCR products of PV insertion into pmCherry N-1.....	34
<u>3.2 -</u> Agarose Gel of pmCherry N-1 Plasmid cleavage by Xho I, BamH I.....	35
<u>3.3 -</u> Results of sequence analysis for PV-mCherry Fusion Plasmid	37
<u>3.4 -</u> Western of CHO with PV-mCherry using Optifect Transfection Reagent.....	38
<u>3.5 -</u> Wide-field fluorescence microscopy of CHO cells transfected with PV-mCherry.....	39
<u>3.6 -</u> Agarose Gel of PCR products of PV-mCherry inserts into α -MyHC.....	41
<u>3.7 -</u> Sequence of α -MyHC PV-mCherry fusion plasmid.....	43
<u>3.8 -</u> Flow Cytometry of CHO cells transfected with CMV and α -MyHC PV-mCherry.....	45
<u>3.9 -</u> Absorption Spectra of CdSe/ZnS in Toluene.....	47
<u>3.10 -</u> Emission spectra of CdSe/ZnS in Toluene.....	47
<u>3.11 -</u> Fluorescence spectra of L-QDs in dH ₂ O.....	48
<u>3.12 -</u> Cryo-EM Image of L-QDs.....	49
<u>3.13 -</u> Wide-Field Fluorescence Microscopy image of CHO cells with L-QD VII.....	50
<u>3.14 -</u> Results of Dynamic Light Scattering of LVII and LQDVII.....	52

<u>3.15</u> - Wide-Field Fluorescence Microscopy of CHO with PV-mCherry using LQDVII.....	53
<u>3.16</u> - Western of CHOs transfected with PV-mCherry plasmid using LQDVII.....	55
<u>3.17</u> - Expression of PV-mCherry in CHO at 24 hours post transfection using LQDA, LQDB, LQDC and LQDVII.....	56
<u>3.18</u> - Expression of PV-mCherry in CHO at 48 hours post transfection using LQDA, LQDB, LQDC and LQDVII.....	57
<u>3.19</u> - Expression of PV-mCherry in CHO at 72 hours post transfection using LQDA, LQDB, LQDC and LQDVII.....	57
<u>3.20</u> - Expression of PV-mCherry in CHO at 96 hours post transfection using LQDA, LQDB, LQDC and LQDVII.....	58
<u>3.21</u> - Expression of PV-mCherry delivered by LQDA at 24, 48, 72 and 96hr time points compared to expression of PV-mCherry delivered by Optifect at 48hrs.....	59

LIST OF ABBREVIATIONS

M	Molarity
C	Degrees Celsius
secs	seconds
mins	minutes
hrs	hours
HF	Heart Failure
LVDD	Left Ventricular Diastolic Dysfunction
PV	Parvalbumin Major Isoform I
mCherry	mCherry Red Fluorescent Protein
PV-mCherry	Parvalbumin – mCherry Fusion protein (CMV promoter)
CMV	Cytomegalovirus (promoter construct)
α -MyHC	Alpha Myosin Heavy Chain (promoter construct)
TH	Thyroxine Hormone (T4)
TRE	Thyroxine Response Elements
QD	Quantum Dot
CdSe/ZnS	Cadmium Selenide Quantum Dots with Zinc Sulfide Shelling
NP	Nanoparticle
L-QD	Liposome-Quantum Dot Hybrid
CHO	Chinese Hamster Ovary cell line
DOPE	18:1 (Δ 9cis) 1,2-dioleoyl-sn-glycero-3-phosphoethanolamine
DC-Chol	3 β -[N-(N',N'-dimethylaminoethan)-carbonyl]cholesterol
DOTAP	18:1 1,2-dioleoyl-3-trimethylammonium-propane
Tris	Buffer of given pH of tris(hydroxymethyl)aminomethane
TBS	Tris Buffer Saline solution
α -MEM	Alpha-Modified Minimum Essential Medium
CCS	Cosmic Calf Serum
PCR	Polymerase Chain Reaction
E.Coli	Escherichia Coli
DLS	Dynamic Light Scattering

ABSTRACT

Left Ventricular Diastolic Dysfunction is one of the main causes of Heart Failure. It is caused by a defect in the relaxation of cardiac muscle usually as the result of failure of the heart cells to remove cytoplasmic Ca^{2+} following muscle contraction. This defect is corrected by the presence of Ca^{2+} sequestering Parvalbumin Major Isoform I (Parvalbumin), a naturally occurring soluble protein in skeletal muscle, which then binds free Ca^{2+} , resulting in increased rates of diastolic relaxation. Since Parvalbumin does not naturally occur in cardiac tissue, ectopic expression through gene therapy provides a vehicle to deliver the gene needed to express this therapeutic protein. This has been accomplished by others using viral vectors but due to the problems associated with viral delivery, non-viral delivery methods are becoming more popular. Cationic Liposomes are a commonly used non-viral method of gene delivery and due to their physical and chemical properties inorganic nano-particles are attracting much interest in the field as well. It is the aim of this research to investigate whether cationic liposomes containing organic-phase fluorescent CdSe/ZnS “quantum dots” can be used as an efficient method of gene delivery into mammalian cells with built-in optical tracers. Organic-phase CdSe/ZnS was synthesized, purified and encapsulated into liposomes using various ratios of 1,2 – dioleoyl – 3 – trimethylammonium – propane (DOTAP), 1,2 – dioleoyl – sn – glycerol – 3 – phosphoethanolamine (DOPE), Cholesterol and 3β – [N – (N', N' – dimethylaminoethan) – carbamoyl] cholesterol (DC-Chol) and used to deliver circular plasmid DNA coding for a Parvalbumin-mCherry fusion protein into Chinese Hamster Ovary (CHO) cells. We are able to show that using this system of cationic liposome-quantum dot hybrids we are able to deliver and express the target gene.

CHAPTER 1: INTRODUCTION

1.1 – Role of Parvalbumin in Correction of Left Ventricular Diastolic Dysfunction

Heart failure (HF) is a common and detrimental form of cardiovascular disease in the United States. The statistics are staggering. For example: 1 in 5 people over 40 will develop this disease in their lifetime; in 2006 it was the primary cause of over 60,000 deaths, 1.1 Million hospitalizations, 3.4 Million ambulance rides and in 2010 HF is estimated to cost Americans 39.2 Billion dollars (Lloyd – Jones, D. et al, 1999).

Left ventricular diastolic dysfunction, a major cause of Heart Failure, is primarily the effect of decreased left ventricular diastolic distensibility (slowed myocardial relaxation). This leads to an increased left ventricular end diastolic pressure (LVEDP) to volume ratio, or simply more pressure is required to achieve the same level of diastolic ventricular volume (Lorell, B., 1991). This slowed myocardial relaxation can be attributed to a number of factors, but it is primarily caused by defects in mechanisms that move intracellular Ca^{2+} from the cytoplasm to the Sarcoplasmic Reticulum during relaxation (mainly active transport via Ca^{2+} ATPase pumps).

It is shown by Wahr et al that the expression of PV in an adenoviral vector can correct diastolic dysfunction in excised rat cardiomyocytes (Wahr, P. et al, 1999). This induced disease state was characterized by a decrease in the rate of fluorescent decay of Fluo-3 AM (a calcium-dependent fluorescent dye) during relaxation, indicating a decrease in relaxation rate due to sustained intracellular Ca^{2+} concentration. After the expression of PV, the rate of fluorescent decay at 37 C° dramatically increased, drastically reducing the time of this Ca^{2+} transient and was done without compromising contraction amplitude. This indicates that through the introduction of Parvalbumin into diseased cardiomyocytes, one can reduce the time of calcium transients, resulting in increased rates of relaxation without reducing systolic contraction.

Having observed PV's efficacy in correcting diastolic dysfunction, Coutu and Metzger later investigated at what level of expression would PV's effect be optimal and what would be the effect of levels being too high or too low? Using both experimental data and mathematical modeling, they determined the effects of a range of PV concentrations in the relaxation rate of excised cardiomyocytes. Experimental data

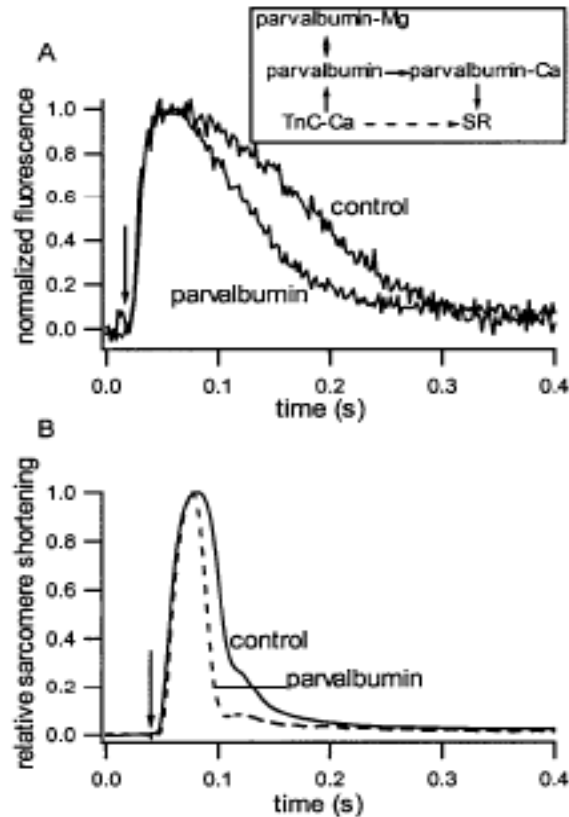


Figure 1.1: Effect of Parvalbumin on the Contractility Rates of Diseased Rat Cardiomyocytes. Figure taken from Wahr et al showing the effect of Parvalbumin on the rates of relaxation of diseased rat cardiac cells. This shows that the expression of PV results in an increase in the rate of fluorescence decay of Fluo-AM, a Ca^{2+} - sensitive fluorescent dye, following contraction of diseased cardiomyocytes. It also shows that there is an increase in the rate of sarcomeric lengthening without any decrease in peak sarcomeric shortening (contractility). Taken together this data suggests that PV can increase the rate of cardiomyocyte relaxation without affecting contractile amplitude (Wahr, P. et al, 1999).

showed that at moderate levels (approximately 0.05mM) PV would effectively buffer Ca^{2+} , increasing relaxation rate without perturbing amplitude. When PV levels are too high (>0.1mM), the relaxation rate increased but the amplitude of contraction diminished. As expected, too low a concentration (<0.01M) had little effect (Coutu, P. et al, 2002). These publications show that PV at the correct concentration range is effective in the correction of diastolic dysfunction. This suggests that the introduction of PV into cardiac tissue may be a potential treatment for this type of dysfunction.

In addition to having an effective method of delivery, it is important to have a safeguard against aberrant expression of gene therapy products, particularly in the expression of Ca^{2+} sequestering proteins like PV, since many bodily processes are highly sensitive to $[Ca^{+2}]$. It is in this line of thinking that the utilization of a cell-specific promoter being employed would be highly valuable. It would assure that should any of gene therapeutics reach any other cell type besides cardiac tissue that they would not express PV, thus providing selective expression.

Robbins and Gulick et al showed that when the entire α -MyHC promoter was coupled with a distal element of the β -MyHC promoter, it was sufficient to drive tissue-specific expression of chloramphenicol acetyltransferase (CAT) in myocardial muscle (Robbins, J. 1997; Gulick, J. et al, 1991). Expression levels in non-cardiac tissue were also tested, finding very low levels of expression in non-cardiac striated muscle tissue and no detection of expression in spleen and uterus smooth muscle as well as liver and kidney non-muscle tissues.

Rindt et al later published research that established the location of two separate and non-equivalent Thyroxine Response Elements (TREs) that regulate transcription through the presence or absence of thyroid hormone (TH) (Rindt, H. et al, 1995). Mutations made in these regions of the promoter vastly affected transcriptional activity, with mutations in each individually leading to distinguishably different levels of expression and mutations in both resulting in little to no transcriptional activity, even in the presence of TH. This implies the possibility, by coupling mutations in TREs with the induction of mild hyperthyroidism (elevation of TH levels in the blood), of using Thyroid Hormone, a naturally occurring hormone, as a pro-drug for the transcription of these cell-specific promoter elements; creating another method of modulating expression.

1.2 – Gene Therapy Techniques and Integration of Nanomaterials

Gene therapy holds the potential to provide a means to cause cardiac muscle to express the protein PV, thus correcting LVDD, a major form of HF. Many forms of gene delivery have been attempted and developed in the past. Previous methods have used primarily viral delivery vehicles and while effective in the delivery of the material in laboratory settings, in clinical applications they show to be problematic (Tripathy, S.K et al, 1996; Bessis, N. et al, 1994). These problems include inflammatory response, immunogenicity, recombination and carcinogenicity. More recently, effective alternatives to viral delivery of genes have been well established. Two such techniques are through the use of cationic liposomes and small inorganic nanoparticles for the delivery of DNA.

One of the best established and reliable non-viral methods of transfecting cells is through the use of cationic liposomes complexed with DNA. Felgner et al synthesized 1,2-di-O-octadecenyl-3-trimethylammonium propane (DOTMA), a cationic lipid, and observed that when combined with equivalent weights of DOPE and liposomes reconstituted in dH₂O these small cationic liposomes readily associated with plasmid DNA. When these complexes were added to CV-7 and COS-7 cells, they were able to observe levels of expression far greater than that of Calcium Phosphate or the DEAE-Dextran transfection techniques. Interestingly, it was noticed that the amount of DNA seemed to have an effective range in transfection efficiency with too much or too little DNA relative to the lipid concentration having an inhibitory effect of the transfection event (Felgner, P. et al, 1997).

Building upon what was observed by Felgner et al, Sakurai et al examined the physiochemical properties as well as the transfection efficiency of DOTMA/DOPE liposomes in various concentrations relative to DNA and found very interesting results. What was observed was that particle size, zeta potential, structure, transfection efficiency and even the distribution in the cell (intracellular trafficking) are all dependent upon the mixing ratios of DNA: Liposomes with a 1: 5 w/w mixing ratio as ideal for most cell types (see **figure 1.2**). At this mixing ratio the amount of Luciferase expression observed is highest, particle size is largest and zeta potential has almost reached its maximum. A very interesting observation in this study is that when higher mixing ratios of lipids are used, the internalization efficiency increases but gene expression is

reduced. Upon using fluorescently labeled DNA and lipids, what was observed was that while the internalization of the higher mixing ratio (1:10) increased, they showed a more punctate localization in the cell, where the the lower mixing ratio (1:5) was more widely dispersed. This suggests that while the internalization of these

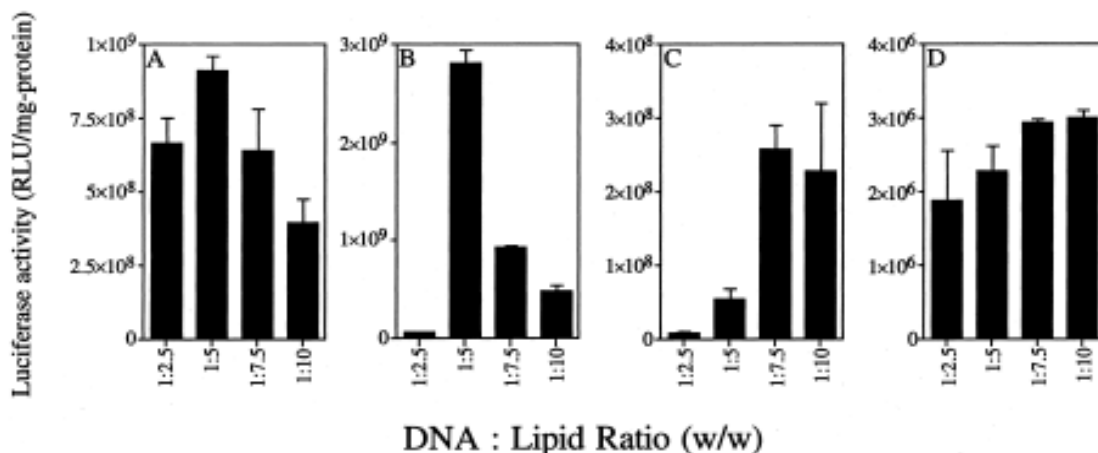


Figure 1.2: Effect of Lipid:DNA Mixing Ratios on the Transfection Rates in Various Cell Lines. Taken from Sakurai et al. Expression of firefly luciferase reporter gene as delivered by different Liposome (1:1 DOTMA:DOPE) to DNA mixing ratios in four different cell lines. From left to right: A) *MBT-2* (mouse bladder tumor) B) *HUVEC* (Human Umbilical Vein Endothelial) C) *NIH3T3* (Mouse Fibroblast) D) *RAW264.7* (mouse macrophage) (Sakurai, F. et al, 2000).

smaller, more positively charged species are readily taken up by the cells, they appear to have problems escaping the endosomes or unpackaging. These finding suggest that the mixing ratio of DNA: Liposomes is paramount in the success of cationic lipid-mediated transfection of DNA (Sakurai, F. et al, 2000).

There has been some concern regarding the use of cationic lipids in gene therapeutics, primarily because of some observed cytotoxicity. Many studies have been conducted on the topic and while cationic lipids have been shown to be slightly cytotoxic, it appears that this can be offset by the incorporation of neutral lipids such as DOPE or DOPC into the liposomes. These lipids, DOPE in particular, have also show to increase efficiency of transfection by disrupting the endosomal membranes (Lv, H. et al, 2006). This same effect, in the increase in transfection efficiency, has also been

observed through the incorporation of Cholesterol and structurally related molecules into cationic liposome formulations (Zidovska, A. et al, 2009).

In recent years, inorganic nanomaterials such as Au, CdSe/ZnS, InP and Fe₃O₄ have been showing promise in the field of medicine, particularly imaging and gene delivery. They have a modifiable surface, making it possible to functionalize them with a number of surface ligands, making their chemical characteristics and biological compatibility very customizable.

They are able to be functionalized with proteins, nucleic acids or any number of thiol or amine-terminating ligands. This has made them very much the subject of interest for cell targeting, imaging and molecular detection (Igor. L, et al, 2005).

As stated before, the surfaces of Quantum dots (QDs) can be manipulated to exhibit any number of surface ligands or functional groups. This has left open the possibility of using several types of coupling mechanisms to attach nucleic acids to the QDs. The two primary methods of coupling have been direct coupling through thiol terminating nucleic acids and electrostatic coupling with positively charged surface ligands like lysine dendrimers and dimethylamino ethane thiol. These complexes have been used to deliver plasmid DNA for trans-gene expression, single-stranded oligo nucleotides for cellular RNA detection and siRNA for endogenous gene knockdown, thus demonstrating their versatility in gene delivery (Ghosh, P. et al, 2008; Oishi, M. et al, 2006; Mitchel, GP. et al, 1999; Li, D. et al, 2008).

Chemical properties and biological compatibility aside, what makes QDs and other nanoparticles so unique are their physical properties. QDs such as CdSe and InP have spectroscopic properties that are vastly superior to typical organic fluorophores. While organic fluorophores have broad excitation and emission spectra and limited resilience to photobleaching and chemical degradation, QDs have broad excitation with very narrow emission spectra that spans the UV to near-infrared region, high molar extinction coefficients (10-100x that of organic dyes) with high quantum yields and exceptional resistance to photobleaching and chemical degradation (Igor, L. et al, 2005). This makes these materials highly valuable as optical tracers in the study of spatial and temporal localization of internalized products. Superparamagnetic Iron Oxide (Fe₃O₄), on the other hand, has no significant optical properties but due to its high magnetic

moment and qualities as an NMR contrast agent, is able to be tracked in a living animal by MRI at very low relative concentrations (Bulte, J. et al, 2004).

The use of QDs and other nanoparticles in medical applications has been subjected to many concerns regarding their toxicity, as Cd^{2+} is known to be toxic in many tissue types, and their fate, as it is not known where they may end up in the body. In recent studies addressing these issues, it is shown that particles 5.5nm or less are renal cleared in the urine (Choi, HS. et al, 2007). Although promising, a more comprehensive study on the effects of QDs in the body over time needed to be undertaken. Hauck et al undertook an investigation to observe the biodistribution, animal survival, animal mass, hematology, clinical biochemistry and organ histology of Sprague-Dawley rats injected with Quantum dots and nanoparticles of various elemental compositions, surface chemistry, sizes and shapes. What they found was that even at high doses and chronic administrations, the rats showed no signs of toxicity, no histological abnormalities, decrease in liver function or any other abnormalities that are outside of standard population variance (Hauck, TS. et al, 2010).

One of the biggest drawbacks in the use QDs for biological purposes is that since most QDs are prepared in the organic phase, surface chemistry must be modified (as discussed earlier) to make them bio-compatible. This process is not only time consuming and challenging, but converting the materials to aqueous phase has a profoundly adverse effect on quantum yield and stability (Kalyuzhny, G et al, 2005). Therefore interest has been taken in methods to use organic phase quantum dots for biological applications.

Recently organic phase QDs such as CdSe/ZnS have been incorporated into the hydrophobic alkyl region of a cationic liposome (composed primarily of DOTAP and DOPE lipids) and that these Liposome -QD hybrids (L-QDs) are able to be internalized into cells and tumors both *in vitro* and *in vivo* (Al-Jamal, WT. et al, 2008). Knowing that this same formulation of lipids is able to deliver and express plasmid DNA and seeing now that it is capable of entrapping and delivering QDs without modification to the QDs surface, it is the intention of this study to develop a method of delivery using L-QDs to bind and deliver DNA into cells. This would provide potent, cheap and easily produced optical tracers of transfection with high stability and a tunable, sharp emission spectra.

1.3 – Aim of Study

It is the intention of this study to combine technologies of cell-specific promoters and lipid-nanoparticle complexes to develop an effective, stable, cell-specific and efficient gene therapy delivery vehicle that can then be applied to the delivery and expression of PV into cardiomyocytes. This can be done through the completion of several steps or benchmarks as follows:

1. **Clone a PV – mCherry (a red fluorescent protein) fusion protein** in a CMV promoter construct (ubiquitous expression vector) and then subsequently clone this fusion protein into a mouse α -Myosin Heavy Chain promoter construct (a promoter which shows cardiac-specific expression). This fusion construct will allow us to visualize the expression of our delivered gene while still in the live cell, thus giving us a convenient means of observing transfection efficiency as well as provide a secondary target for immunodetection (Western Blot detection of mCherry). After completion of the primary cloning, we want to test the functionality of these constructs by transfection into Chinese Hamster Ovary using commercially available cationic liposome transfection reagents. This will be done to check the discriminatory expression pattern of α -MyHC promoter vs CMV promoter.
2. **Synthesize CdSe/ZnS quantum dots, incorporate them into the alkyl region of the lipid bilayer of a cationic liposome and use these liposomes for the transfection of DNA into mammalian cells.** These quantum dots will provide for us an optical tracer, allowing us to visualize microscopically the internalization of the lipid-DNA complexes. Therefore we can track the localization of our gene therapy drugs without modifying our DNA or lipids with fluorescent markers or dyes. These L-QDs will be delivered into the immortal cell lines CHO and optimized by using various combinations of cationic and neutral lipids as well as investigating the effect of L-QD:DNA ratio on transfection efficiency and robustness of expression.

CHAPTER 2: METHODS AND MATERIALS

The goal of this project, as stated previously, is to deliver a Parvalbumin-mCherry Fusion peptide into mammalian cells using cationic liposome – Quantum Dot hybrids (LQDs). For the purposes of methodology, this project can be thought of as the culmination of three individual efforts: Cloning, Preparation of Materials and Mammalian Cell Culturing. Although it is primarily a three pronged effort, each facet or step of this study will be presented individually.

2.1– Cloning of PV onto N-terminal of mCherry (CMV)

The initial step in cloning of the PV-mCherry fusion peptide was to perform a PCR of my Parvalbumin gene (obtained from Dr. Moerland, FSU) so as to add a Xho I restriction site onto the 5' end (as well as an secondary Sal I restriction site slightly downstream of Xho I for the purposes of future cloning into α -MyHC promoter plasmid) and a Hind III restriction site onto the 3' end. This initial PCR was performed by adding 3 μ L (58.6 ng/ μ L) Parvalbumin Major Isoform I in pCR 2.1 – TOPO vector (Invitrogen) to a 0.5mL PCR eppendorf tube containing 45 μ L PCR Supermix (Invitrogen) with 1 μ L forward primer PVpmCN1scmodf (**Figure 2.1a**) and 1 μ L reverse primer PVpmCN1scR (**Figure 2.1b**); both primers being 100 μ M in concentration. This solution was then placed into a PCR Thermocycler programmed accordingly:

- 1) Initial Denature – 95C, 5 mins
- 2) Cycle 35 times
 - a) Denature – 94C, 1 min
 - b) Anneal – 58C, 45 secs
 - c) Elongate – 72C, 1 min
- 3) Final Elongation – 72C, 10 min
- 4) Hold – 4C, indefinite

The success of this PCR is then tested Agarose Gel Electrophoresis in order to identify a band of approximately 330bp. This was performed by first mixing 10 μ L of the

reaction with 2µL 6x loading buffer and loaded onto a 0.8% agarose gel (0.4g Electrophoresis Grade Agarose, 50mL 1x TAE buffer) in 1x TAE buffer and run at 80V for 90 mins.

6x DNA Loading Buffer

40% Sucrose

0.25% Bromophenol Blue

1x TAE Electrophoresis Buffer

40mM Tris-Acetate

1mM EDTA

PVpmCN1scmodf

5' – TCA GAT **CTC GAG** CTC CTG CAG **TCG ACG** GTC **GCC ACC ATG** **GAT ATT ACA**
GAT GTG CTT GCC – 3'

Blue = Xho I restriction site

Green = Acc I / Sal I restriction site

Orange = Kozak sequence translation initiation site

Red = Anchor Sequence to Parvalbumin

Figure 2.1a: 5' PCR forward primer for the production of PV-mCherry fusion protein. Contains Xho I and Acc I/ Sal I restriction sites, the Kozak sequence and a 20bp anchoring sequence for Parvalbumin Major Isoform I.

PVpmCN1scR

5' – GGC CCG TGG ATC CCG GGC TGC TTG ACC TAC GAG GTT GAC AAA – 3'

Fuchsia = BamH I restriction site

Red = Anchoring Sequence

Figure 2.1b: 3' PCR reverse primer for the production of PV-mCherry fusion protein. Contains a BamH I restriction site and a 24bp anchoring sequence for Parvalbumin Major Isoform I.

Once the gel has finished running, it is then stained with 1x SYBR Gold (Molecular Probes, Invitrogen, Carlsbad, California) DNA stain in 1x TAE buffer and imaged using a Bio-Rad Molecular Imager Gel Doc XR+ System (Life Science, Hercules, California). Upon visualization of the appropriate sized band, the PCR product was then purified using a PCR Cleanup Kit (Qiagen, Valencia, California) according to manufacturer protocol.

Following successful PCR and purification, the PCR products and pmCherry-N1 plasmid (Clontech, Mountain View, California) must then be cleaved by Xho I and BamH I restriction enzymes so that they contain complimentary ends for ligation. This is performed by adding plasmid and PCR products to the following reaction formulations in 0.5mL eppendorf tubes:

Plasmid Restriction Digest

- 1) 5µL plasmid pmCherry-N1
- 2) 5µL 10x React 2 NEB buffer
- 3) 38µL dH₂O
- 4) 2µL XhoI enzyme
- 5) 2µL BamHI enzyme

PCR Restriction Digest

- 1) 40 μ L PCR Product
- 2) 5 μ L 10x React 2 NEB buffer
- 3) 3 μ L dH₂O
- 4) 2 μ L Xho I enzyme
- 5) 2 μ L BamH I enzyme

These restriction digest reactions are then placed into a 37C water bath to optimize the activity of the restriction endonuclease enzymes and the reactions allowed to incubate for 1 – 2 hrs. As before with the PCR reaction, following digestion, these reactions must be purified for ligation. This is done same as before by using a PCR Cleanup Kit and the concentrations tested. Once purified, the cleaved PCR product of Parvalbumin Major Isoform I can then be combined with the cleaved and purified pmCherry N-1 plasmid for ligation using T4 DNA Ligase (New England Biolabs Inc, Ipswich, Massachusetts) . This reaction vessel is prepared as follows:

Ligation Reaction

- 1) 13 μ L pmCherry-N1 (6.5ng/ μ L)
- 2) 1.5 μ L PV PCR insert
- 3) 2 μ L 10x Ligase Buffer
- 4) 1 μ L T4 Ligase Enzyme
- 5) 3 μ L dH₂O

Ligation reaction is then allowed to incubate protected from light at 25C overnight. Following ligation, the cloned plasmid must be transformed into bacterial cells (using heat-shock transformation method) for future proliferation and preparation. This is performed by first diluting this reaction 5x with dH₂O to a volume of 100 μ L. To 100 μ L chemicompetant DH5 α cells on ice 1 μ L of the diluted ligation reaction is then added. This mixture is then placed on ice and allowed to incubate for 1hr. Following this 1hr incubation, the cell suspension is heat shocked at 42C for 45secs. Immediately

following heat shock, the suspension is then placed onto ice for 2mins, at which time 900 μ L SOC media (without antibiotics) is added. This SOC media cell suspension is then placed into a culture tube and incubated in a shaker at 37C for 2 hours to improve the health of the heat-shocked culture.

In order to isolate transformed, PV-mCherry containing bacteria from those that have not, 70 μ L of the culture is streaked onto Kanamycin LB Agar plates (30 μ g/mL) and the plates placed into a 37C incubator overnight. Those individuals that received the cloned plasmid will retain a Kanamycin-resistance gene and be able to proliferate on these plates while those that did not receive the plasmid will not. The following morning, several individual colonies were then ex-planted and placed into separate culture tubes containing 5mL LB with 30 μ g/mL Kanamycin and allowed to grow overnight in a 37C shaker. At this point, some of the culture must be used to preserve the bacterial stock while the rest is used for plasmid extraction for sequence analysis.

For stock preservation, 700 μ L of the saturated culture was combined with 300 μ L 100% glycerol, mixed well and frozen at -80C. The remainder of the suspension was centrifuged to a pellet and supernatant removed. Plasmid was extracted using a Miniprep Plasmid Extraction Kit (Qiagen, Valencia, California) according to manufacturer protocol. The extracted plasmid is then resuspended in dH₂O at a concentration of approximately 100 μ g/ μ L for sequencing. Primers used for sequencing were complimentary to the PV portion of the fusion gene and designed to read well into the promoter in the 5' direction and well past the mCherry gene in the 3' direction. Sequences were then analyzed to see which gene sequences are correct.

2.2– Site Directed Mutagenesis to Remove Internal Kozak Sequence of PV-mCherry

Section 2.1 discussed the preparation of a fusion peptide between Parvalbumin Major Isoform I and mCherry Red Fluorescent Protein. Once successfully cloned, this will result in a fusion construct that will express with a CMV promoter and relies on the heavily conserved Kozak sequence for ribosomes to initiate translation. In the initially cloned plasmid, however, there will be two Kozak sequences, one at the 5' of PV and

another at the 5' of mCherry. This presents the possibility for multiple initiation sites for the ribosome to begin translation. Since the immunodetection and visualization of mCherry is essentially how the expression of PV is to be observed and quantified, it is imperative that only the fusion protein and not the uncloned mCherry be expressed. With that in mind, the removal of this internal Kozak must be accomplished via Site-Directed Mutagenesis.

This procedure is taken from the Quickchange Site-Directed Mutagenesis Kit (Stratagene, Agilent Technologies Inc, Santa Clara, California) and begins with the preparation of a PCR reaction:

SDM Reaction Solution

- 1) 5 μ L 10x rxn buffer
- 2) 1 μ L Template Plasmid
- 3) 1 μ L Forward Primer (SDMKozakpmcn1f, **Figure 2.2**)
- 4) 1 μ L Reverse Primer (SDMKozakpmcn1r, **Figure 2.2**)
- 5) 1 μ L dNTP mixture
- 6) 1 μ L Pfu turbo DNA polymerase enzyme
- 7) 40 μ L dH₂O

SDMKozakpmcn1f

5' - GAT CCA CCG GTC GCG GCC ATG GTG AGC AAG – 3'

Light Blue = Double Mutant

SDMKozakpmcn1r

5' – CTT GCT CAC CAT GGC CGC GAC CGG TGG ATC – 3'

Light Blue = Double Mutant

Figure 2.2: Primers used for SDM of PV-mCherry Fusion to remove internal Kozak sequence. These two primers are used for the Site-Directed Mutagenesis of the PV-mCherry fusion protein to remove the internal Kozak sequence that lies in the spacing between Parvalbumin and mCherry in the fusion construct. Normally C GCC ACC ATG G, these primers change it into C GCG GCC ATG G.

Once mixed, this PCR reaction is then placed into a thermocycler that is operated under the following program:

SDM Thermocycler Program

- 1) Initial Denature – 95C, 2mins
- 2) 18 Cycles
 - a) Denature – 95C, 30secs
 - b) Anneal – 55C, 1min
 - c) Elongate – 68C, 5mins
- 3) Final Elongation – 68C, 10mins
- 4) Hold – 4C, indefinite

Following the PCR reaction, the mutated plasmid must be differentiated from the original plasmid. To do so, the endonuclease enzyme Dpn I, that digests only methylated DNA, is employed to chew up all methylated, un-mutated plasmid. This is performed by the addition of 1µL of Dpn I to the PCR reaction vessel. This solution is

then incubated at 37C for a minimum of 1hr to digest the original plasmid. Following this digestion, only the DNA of interest remains. This plasmid is then transformed into DH5 α E.coli cells, plated and colonies selected as described previously. Selected colonies are then grown, plasmid isolated and submitted as described previously.

2.3 – Sub-Cloning of PV-mCherry into α -MyHC Cardiac-Specific Promoter

In this section, the PV-mCherry is to be sub-cloned into α -MyHC for the purpose of producing a cardiac-specific plasmid that coded for the expression of PV-mCherry fusion peptide. Due to the organization of the α -MyHC plasmid (obtained from and designed by Dr. Jeffrey Robbins, University of Cincinnati) only two restriction sites are available for exploitation: Sal I and Hind III. Normally this would be a straight-forward cloning procedure but since PV has an internal cut site for Hind III, either Sal I needs to be employed on both ends of the insertion gene or some other strategy formulated. After multiple unsuccessful efforts to clone PV-mCherry into α -MyHC utilizing Sal I on both 5' and 3' ends of the PV-mCherry insert, it was determined that a mutation in the PV-mCherry gene to remove the Hind III cut site followed by a direct insertion cloning method would be the most likely to succeed. So keeping in line with this strategy, the first procedure undertaken is a PCR to create a mutated PV-mCherry protein that would have the Hind III cut site removed without changing the amino acid sequence (GGA \rightarrow GGG mutation in reading frame, both code for Glycine). The following reaction was prepared in a 0.5mL eppendorf:

Site-Directed Mutagenesis PCR Reaction of PVmCherry to Remove Internal Hind III Cut Site

1 μ L DNA Plasmid PVmCherry (with removed internal Kozak)

1 μ L Forward primer (SDMpvmcn1hindiif, **Figure 2.3**)

1 μ L Reverse Primer (SDMpvmcn1hindiir, **Figure 2.3**)

5 μ L 10x Reaction Buffer,

40 μ L dH₂O

1 μ L dNTP Mix

1 μ L pfu Turbo Enzyme

SDMpvmcn1hindiif

5' – CAA TTT CCA AAA GCC CGG **G**AG CTT CAA TCA CAA GGT GT – 3'

Light Blue = A → G Point Mutation to Remove Hind III restriction site (AAGCTT)

SDMpvmcn1hindiir

5' – ACA CCT TGT GAT TGAAGC **T**CC CGG GCT TTT GGAAAT TG – 3'

Light Blue = T → C Point Mutation to Remove Hind III restriction site (AAGCTT)

Figure 2.3: Primers used to remove Hind III cut site in Parvalbumin Gene via SDM. Each contain a single point mutation at the beginning of the Hind III restriction site.

This reaction was then placed into a thermocycler as previously described and run on the following temperature program:

SDM Thermocycler Program to Remove Hind III Cut Site from PVmCherry

- 1) Initial Denature – 95C, 5mins
- 2) 15x cycles
 - a) Denature – 95C, 1min
 - b) Anneal – 61C, 1min
 - c) Elongation – 68C, 6.5mins
- 3) Final Elongation – 68C, 10mins
- 4) Hold – 4C, indefinite

In a method exactly the same as that described in the digestion of PCR products from SDM of the internal Kozak sequence of PV-mCherry fusion peptide, the contents of the SDM PCR reaction to remove the Hind III cut site were then cleaved with DpnI for 1-2hrs, transformed into DH5α cells and streaked onto Kanamycin LB Agar plates.

Colonies were then isolated and grown up; plasmid extracted and sequenced. Once the correct sequence was identified, sub-cloning into α -MyHC was performed exploiting Hind III and Sal I restriction sites.

PCR Reaction of PVMCherry into α -MyHC

1 μ L PVMCherry (internal kozak sequences and HindIII sites removed)

1 μ L forward primer (PVpmCN1scmodf, **Figure 2.1a**)

1 μ L reverse primer (α MyHCscPVpmCN1r, **Figure 2.4**)

47 μ L PCR Supermix

Thermocycler Program for PCR of Sub-Cloning of PVMCherry into α -MyHC

- 1) Initial Denature – 95C, 5mins
- 2) 35x cycles
 - a) Denature – 95C, 45secs
 - b) Anneal – 63C, 45secs
 - c) Elongation – 72C, 2mins
- 3) Final Elongation – 72C, 10mins
- 4) Hold – 4C, indefinite

α MyHCscPVpmCN1r

5' - GGA TCT **AAG CTT** CCG **CTA** **CTT GTA CAG CTC GTC CAT GCC** - 3'

Green = Hind III restriction site

Blue = Stop Codon

Red = Anchoring Sequence

Figure 2.4: Reverse primer for PCR PV-mCherry subcloning into α -MyHC cardiac-specific promoter. Contains Stop Codon, Hind III restriction site and 21bp anchoring sequence.

As with the previous cloning procedure described in section 2.1, the resulting PCR amplification is characterized by Agarose gel electrophoresis. Following characterization, the PCR is then purified using a PCR Clean-Up Kit (Qiagen). Once purified, the PCR insert and the α -MyHC plasmid are then both cleaved with Sal I and Hind III enzymes. In this case however, the two restriction digestion reactions occur separately, with purification steps between them. The initial Sal I digest was prepared in a 0.5mL eppendorf tube with the following formulation:

Sal I Restriction Digest of PCR Reaction

40 μ L PvmCherry PCR reaction
5 μ L 10x React 10
1 μ L Sal I enzyme
4 μ L dH₂O

Sal I Restriction Digest of α -MyHC

5 μ L α -MyHC Plasmid
5 μ L 10x React 10
1 μ L Sal I enzyme
39 μ L dH₂O

Both of these reaction tubes were then placed into 37C water baths for 2hrs. Afterward, the DNA from these digests was recovered by 70% Ethanol Precipitation in the presence of 200mM NaCl and 10mM MgCl₂. This solution containing DNA, salts and ethanol was cooled at -20C for 30 mins then centrifuged at maximum velocity for 20mins at 0C. Pelleted DNA is then re-suspended in 50 μ L 10mM NaCl, 10mM Tris pH 7.5. The recovered DNA was then digested by Hind III enzyme in the following reaction formulation:

Hind III Cleavage of Sal I – Digested PV-mCherry PCR, α -MyHC Plasmid

44 μ L cut α -MyHC and PV-mCherry recovered from Sal I digest, respectively

5 μ L 10x React 2 Buffer

1 μ L Hind III enzyme

This reaction was then incubated at 37C for 2hrs. Following secondary digestion, the products of the cleavage reaction are then purified again by Ethanol Precipitation as described previously. Once purified and re-suspended into 50 μ L 10mM NaCl, 10mM Tris pH 7.5 buffer, the inserts and plasmid were then combined and ligated using T4 Ligase as described:

α -MyHC PVMCherry Ligation Reaction

2 μ L 10x Ligation Buffer

1 μ L T4 DNA Ligase

11 μ L double digest PCR of PV-mCherry

6 μ L α -MyHC double digest

This ligation reaction was allowed to proceed overnight at room temperature protected from light. The following day, this reaction was diluted 5x and transformed into DH5 α cells as described previously. Following streaking onto Ampicillin LB Agar plates (α -MyHC plasmid contains an Ampicillin-resistance gene), selection and growth of colonies, plasmid was extracted and purified as described previously. The sequence of those samples were then analyzed.

2.4 – Preparation of CdSe/ZnS Quantum Dots

As stated before, the incorporation of organic-phase inorganic Quantum Dots into cationic liposomes for the purposes of gene delivery is the goal of this study. The first step in creating these hybrids is the synthesis of the QDs themselves. This is done in two steps: the synthesis of the fluorescent core nanoparticle CdSe followed by the ZnS shelling of the CdSe to create CdSe/ZnS.

The core CdSe quantum dots are prepared using a microwave method

developed by Dr. Aaron Washington and Dr. Geoffrey Strouse. A 10mL static vessel containing 4mL 50mM Cd Stearate ($\text{Cd} [\text{CH}_3(\text{CH}_2)_{16}\text{COOH}]_2$) in Decane, 600 μL 1M Selenium powder in Tri-octyl Phosphine ($[\text{CH}_3(\text{CH}_2)_7]_3\text{P}$) and a stir bar was fitted with a pressure cap and placed into a CEM Discover System. This system was then operated at 300W, 2.45GHz under pressure until a holding temperature of 160C was reached. This growth temperature was then maintained by the system for 45secs followed by rapid cooling using high pressure air (40psi).

Now that the reaction is completed and the core CdSe synthesized, the solution must be cleaned of any un-reacted reagents and size-selective precipitation performed to isolate as uniform a population of particles as possible. This is accomplished by first cooling the reaction to room temperature and spinning at maximum velocity in a swinging-bucket rotor centrifuge for about 10 minutes to pellet out un-reacted, insoluble reagents and the supernatant pooled. The supernatant contains the particles of interest, which are green-emitting QDs of approximately 3.5nm in diameter. To this suspension is then added a mixture of 1-Butanol and Methanol until the first signs of aggregation is observed (as indicated by a cloudiness in the solution). This suspension is then centrifuged again in a swinging-bucket rotor at maximum velocity for approximately 10 minutes. After centrifugation, the supernatant is transferred to a new vessel. This first precipitation step is to remove the largest particles in the mixture as they will precipitate first. The supernatant, which still contains our particles of interest, is then treated further with additional Methanol to precipitate out the remaining QDs and centrifuged again. Following this step, the pelleted QDs are re-suspended in a small volume (~5mL) of Toluene and sonicated to break up any aggregates that have formed during the precipitation process. They are then crashed out again with Methanol and spun out as before. This process is repeated 3 to 4 more times in order to clean the materials as best as possible. Once sufficiently cleaned and re-suspended in toluene, the absorption and emission spectra are then measured on a Cary 50 Bio Uv-Vis Spectrophotometer and Cary Eclipse Fluorescence Spectrophotometer (Varian, Agilent Technologies, Palo Alto, California), respectively. At this point once satisfactory core materials have been produced and isolated, the process of ZnS shelling can begin.

The procedure for ZnS shelling in the presence of Tri-octyl Phosphine Oxide

(TOPO, $[\text{CH}_3(\text{CH}_2)_7]_3\text{PO}$) is one that was taken from a paper published by Dabbousi et al. In a tri-neck flask we place appropriate fittings for a single N_2 / vacuum line, a 400C mercury thermometer and a single rubber septum for the addition of reagents. In this flask we place a stir bar and 10g of solid TOPO. A heating mantle and stir plate are then placed underneath the flask and the TOPO is melted under vacuum while stirring. The temperature is then raised to 190C and held at this temperature under vacuum for about 2hrs. At this time, the temperature is reduced to 65C; 1mL of pure Tri-octyl Phosphine and clean CdSe in Toluene, prepared from the microwave reaction procedure described above, are added. The temperature is then held around 90C under a N_2 stream 30mins to remove the Toluene from the reaction vessel. The temperature is then ramped up to and held at 160C, at which point 10mL of a solution containing 300 μL dimethyl zinc ($\text{Zn}(\text{CH}_3)_2$), 125 μL hexamethyldisilathiane $(\text{CH}_3)_6\text{Si}_2\text{S}$ and 9.6mL Tri-octyl Phosphine are added drop-wise to the reaction vessel. Immediately after the addition of the ZnS capping reagents, the temperature is reduced to 90C under ambient N_2 and allowed to remain at this temperature for 4 hrs to facilitate the completion of the shelling process. The heat source is then removed and 5mL 1-Butanol added to prevent solidifying of TOPO in solution upon return to room temperature. The solution is allowed to remain stirring overnight (protected from light) until completely cooled. This "mother liquor" is then stored under N_2 , protected from light at room temperature. For all subsequent applications, QDs need to be cleaned by Methanol precipitation. An aliquot of this mixture is then diluted 3x with Toluene and Methanol is added slowly until the very first signs of precipitation. It is then centrifuged, the supernatant removed and the pellet re-suspended in Toluene. Excessive Methanol addition should be avoided. Absorption and Emission Spectra is then collected to determine size and concentration of the QDs.

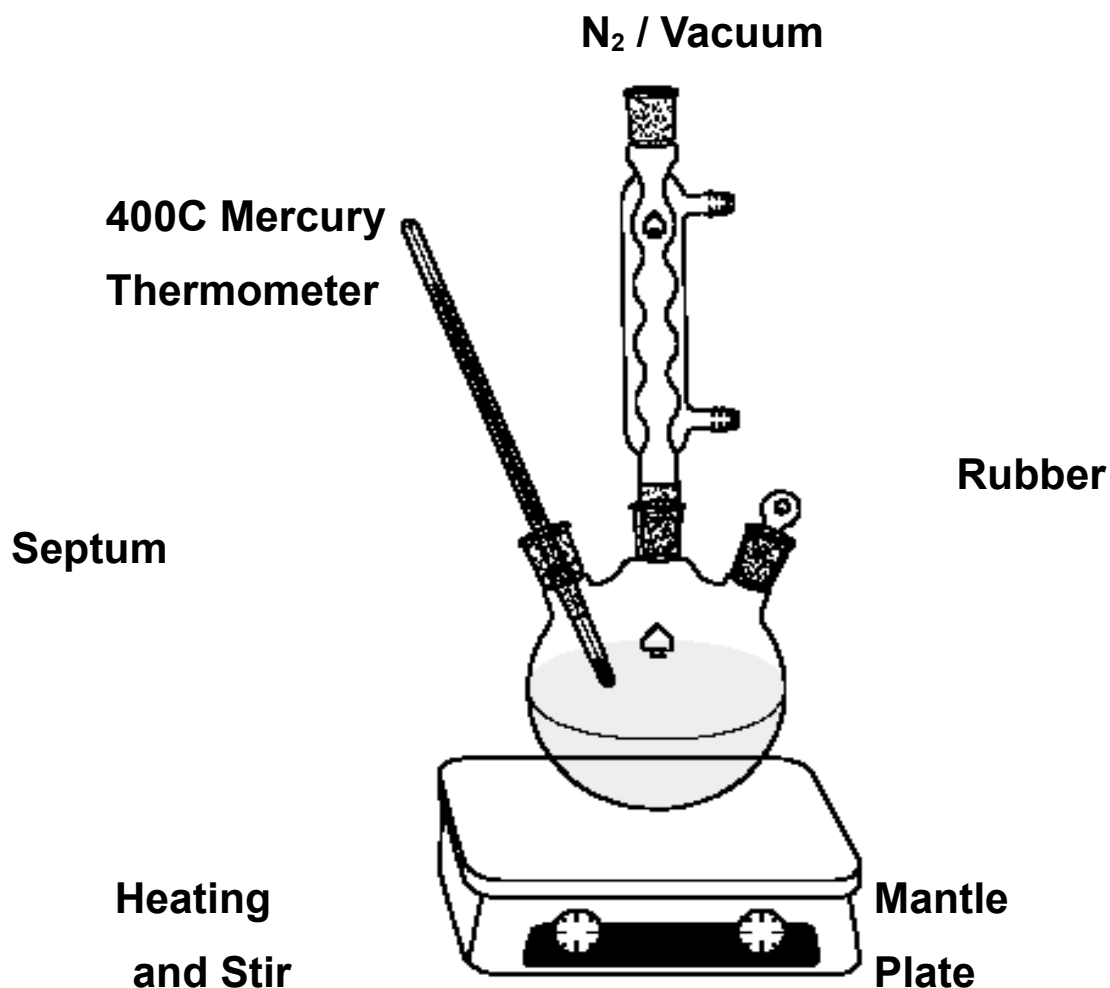


Figure 2.5: Typical arrangement of 3-Neck Flask synthesis vessel used for ZnS shelling. Heating Mantle is not shown in this figure but would normally lie on the top of the stir plate.

2.5 – Encapsulation of Organic-Phase CdSe/ZnS into Cationic Liposomes

Now that the organic-phase CdSe/ZnS has been prepared and characterized by absorption and emission spectra, it can be incorporated into cationic liposomes. First, CdSe/ZnS QDs need to be cleaned and re-suspended in Toluene as described above. The concentration of the CdSe/ZnS is determined by measuring the absorption at its characteristic exciton (which is indicative of the particles size with larger QDs having higher wavelengths of absorption). For QDs grown at 160C a peak in absorption around 525nm (**Figure 3.9**) and emission maximum around 550nm (**Figure 3.10**) is

observed. Using Beer's Law, the concentration of the QD solution can then be determined. For particles of this size, an extinction coefficient (ϵ) of approximately $1 \times 10^5 \text{ A/cm}^2 \cdot \text{M}$ can be used:

$$A = \epsilon b C \rightarrow C = A/\epsilon b$$

Once clean and of known concentration, QDs are ready to be incorporated into cationic liposomes using a slightly modified procedure taken from Al-Jamal et al. The best results were obtained when 1.43×10^{-9} moles of CdSe/ZnS were dried under an N_2 stream for approximately 2 hrs (making sure to sonicate just prior to drying to break up any aggregation that may have occurred during the cleaning process). Once all Toluene is removed, $300 \mu\text{L}$ of 20 mg/mL lipid solution in CHCl_3 is added to the dry QD film. The QDs quickly disperse in CHCl_3 and should be sonicated again briefly. The CHCl_3 is then dried from the sample by the application of an N_2 stream as described previously. After all solvent appears to be dry, the vessel is then sealed tightly and a vacuum applied overnight to remove as much solvent as possible. Once dry, this film can be stored under N_2 at -20C (protected from light) for extended periods of time without any notable loss in fluorescent intensity.

The reconstitution of the Quantum Dot Liposome Hybrids (L-QDs) is performed by first heating the dry L-QD film in the test tube via 80C water bath. After 1-2 mins, the tube is removed from heat and 1.5 mL of filtered, autoclaved dH_2O is added and mixed vigorously to re-suspend the dried film. Once re-suspended, the mixture should appear very cloudy. This mixture is then sonicated vigorously for 10mins until all aggregates have been broken up. This should reveal a solution that is very slightly opaque but translucent. The solution is then collected into a syringe and passed through a $0.2 \mu\text{m}$ syringe filter. This solution should be clear with a slight orange-pink hue. This now contains the finished L-QD products.

Now the finished products need to be checked for fluorescence and the concentration determined. The fluorescence of this solution can then be checked using a Carey Eclipse Fluorescent Spectrophotometer with excitation of 350 nm to confirm the presence of QDs within the liposome solution. The fluorescent signal should produce a

peak at exactly the same wavelength as prior to incorporation into the liposome (**Figure 3.11**). Using these quantities of lipids and dH₂O, the resulting lipid concentration should be approximately 4mg/mL. The concentrations of these resulting solutions is determined by difference in mass measurements of a test tube. A 1.5mL eppendorf tube is weighed (to the 0.0001g) three times and averaged. 0.5mL of the L-QD solution is then added to the eppendorf tube and dried via speed-vac overnight. The following day, the same eppendorf tube with L-QD film residue is weighed again three times and averaged. The difference in mass is the mass of the L-QD film.

$$\text{Mass}_{\text{final}} - \text{Mass}_{\text{initial}} = \text{Mass}_{\text{L-QD}}$$

2.6 – Cell Culture and Transfection Experiments

While the bulk of the work has been in the production of the cloned PV-mCherry fusion peptide, its sub-cloning into the α -MyHC and the successful production of the the L-QD hybrids, it remains the aim of this study to observe their efficacy in delivering and expressing their target gene within mammalian cells. Chinese Hamster Ovary (CHO) cells were chosen because the Strouse and Logan Labs have extensive experience working with these cells, they were readily available in the Protein Expression Facility in Florida State University's Institute of Molecular Biophysics (operated by Dr. Joan Hare), they grow in monolayers (which is more similar to most physiological tissue than are suspension cell lines), they are extremely vital, easy to proliferate and exhibit robust expression of transgenes.

CHO cells were taken from thaw and grown up in α -MEM media supplemented with 10% Cosmic Calf Serum (CCS) (Hyclone, Logan, UT), 0.1% Antibiotic/Antimycotic cocktail (10,000 units of penicillin, 100 ug of streptomycin and 25 ug amphotericin B [Invitrogen/Gibco, Carlsbad, CA]), 0.01% Gentimycin (Invitrogen/Gibco) in a 25cm² culture flask (Corning Incorporated Life Sciences, Santa Cruz, CA) in a 37C, 5% CO₂ incubator. Upon reaching confluency, cell monolayers were washed 1x with TBS, trypsinized with Trypsin-Like Enzyme (TLE) (Invitrogen/Gibco) and taken up in 1mL antibiotic/antimycotic (AB/AM) – free media. CHO cell concentration and viability are then determined using a Cedex HiRes Cell Analyzer (Innovatis AG Inc, Malvern, PA)

according to manufacturer's protocol.

For transfection experiments, cells were either seeded into 6 well (10cm²) or 24 well (2cm²) plates. After counting, cells were then seeded into wells containing AB/AM – free media (3 x 10⁵ cells, 2mL media per 6 well plates [10cm²] and 6 x 10⁴ cells, 0.5mL media per 24 well plates [2cm²], both from Corning Incorporated Life Sciences) and allowed to adhere for 24hrs, this resulted in approximately 70% confluency for the day of transfection.

In transfection experiments utilizing Optifect as the DNA delivery reagent, transfections were performed as prescribed by the manufacturer protocol. DNA and Optifect are added to AB/AM, serum – free media in separate containers (15µL optifect, 4µg DNA in 0.5mL media for 10cm² wells, 2µL optifect, 1µg DNA in 100µL media for 2cm² wells). The two mixtures were combined and allowed to associate for about 30mins. The combined mixtures were then added to the appropriate wells. The cells were then incubated for 6hrs with the transfection reagent/DNA mixture. At that time the media was removed, cells were washed 1x with TBS and fresh, complete media was added.

Transfection experiments utilizing L-QDs were performed in an almost identical fashion. DNA and L-QDs were combined with AB/AM, serum – free media in separate containers. The two solutions were then combined and allowed to associate for 30 mins prior to addition to the cell monolayers. Unless specified otherwise, reagents were mixed in a 5:1 w/w ratio of L-QDs:DNA.

Cells were typically allowed 48 hrs to express the transgene before being imaged, harvested or trypsinized. For experiments spanning longer than 48 hrs, cells were cut back to 50% confluency every 48 hrs by trypsinization with TLE as described above to reduce stresses induced by over-confluency as much as possible.

2.7 - Western Blot Analysis

Western blots were the primary method of quantifying the amount of protein produced by the cells transfected with PV-mCherry. As stated previously, typically the cells were harvested 48 hrs post transfection. At this point, cells ready for harvest were washed 1x with TBS and then lysed using Eukaryotic Lysis Buffer (500µL for 10cm² and

100 μ L for 2cm²).

Eukaryotic Lysis Buffer

- 1) 150mM NaCl
- 2) 50mM Tris – HCl pH 7.6
- 3) 1% Triton X – 100
- 4) 2mM EDTA
- 5) 1mM Na₃VO₄
- 6) 1mM DTT
- 7) 0.1% SDS
- 8) 0.01% Saponin
- 9) 0.5% Sodium Deoxycholate
- 10) 100 μ M EG4
- 11) 50 KIU/mL Aprotinin

Once collected, the cell lysate was then concentrated using Amicon Ultra 0.5mL 10kMWCO (1 x 10⁵ Da Molecular Weight Cut Off) Ultracel Regenerated Cellulose concentrator spin columns (Amicon, Millipore, Billerica, Massachusetts) to approximately 1/3 original volume. Equivalent volumes of sample and 2x Protein Sample Buffer are combined and heated at 90C for 5 – 10 mins and then centrifuged briefly to recover any water droplets that may have formed.

2x Protein Sample Buffer

100mM Tris – HCl pH 6.8
200mM Dithiothreitol
4% SDS
0.2% bromophenol blue
20% Glycerol

Samples were then loaded into 10% SDS-PAGE Glycine Gels with 4% Stacking Gels (10 μ L for 15 well gels, 20 μ L for 10 well gels) and run at 100V for 15 mins followed

by 130V for 90 mins alongside a size marker (Magic Mark, Invitrogen).

10% SDS – PAGE Separating Gel (10mL)

- 1) 4.05mL dH₂O
- 2) 2.5mL 1.5M Tris – HCl pH 8.2
- 3) 100µL 10% SDS in dH₂O
- 4) 3.3mL 30% Acrylamide/Bis-Acrylamide (29:1)
- 5) 50µL 10% Ammonium Persulfate (APS)
- 6) 15µL Tetramethylethylenediamine (TEMED)

4% SDS – PAGE Stacking Gel (5mL)

- 1) 3.05mL dH₂O
- 2) 1.25mL 0.5M Tris – HCl pH 6.8
- 3) 50µL 10% SDS
- 4) 0.66mL 30 Acrylamide/Bis-Acrylamide (29:1)
- 5) 37µL 10% APS
- 6) 10µL TEMED

1x Glycine Running Buffer

14.4g Glycine
3g Tris Base
1g SDS
dH₂O up to 1L

Following gel electrophoresis, the separated proteins must be transferred onto a membrane which can then be used for immunodetection. This is accomplished by preparing a typical Western Blot Wet–Tank Transfer “sandwich” apparatus (**Red** (positive pole); clear plate; pad; 3MM blot paper; membrane; gel; 3MM blot paper; pad; black plate; **Black** (negative pole)). The gel is placed alongside a depolarized Polyvinylidene Difluoride (PVDF, 0.45µm pore size, Immobilon, Millipore) membrane. This membrane is depolarized by first washing it in 100% Methanol for 5 mins. It is then

submerged into 1x Transfer Buffer along with the 3MM blot paper and the transfer pads. The apparatus is assembled then submerged into cold (4C) 1x Transfer Buffer and run at 100V for 1hr whilst the buffer is kept stirring; using a salted ice bath to keep solution cool.

1x Transfer Buffer (1L)

- 1) 10% Methanol
- 2) 3.03g Tris – Base
- 3) 14.4g Glycine
- 4) dH₂O to 1L

Once the transfer is complete, the membrane must be “blocked”. This will prevent non-specific interaction between the primary antibody and the proteins on the surface of the membrane. The membrane is submerged in Blocking Buffer for 1hr at 25C (or overnight at 4C) on a shaker, allowing the buffer to sufficiently move across the entire membrane's surface.

Blocking Buffer (50mL)

- 1) 2.5g Powdered Non-Fat Milk
- 2) 1% Bovine Serum Albumin (optional)
- 3) 1x Rinse Buffer to 50mL

1x Rinse Buffer (1L)

10mM Sodium Phosphate pH 7.2

1% NaCl

0.05% Tween – 20

Following the blocking procedure, the blot is then exposed to a Primary Antibody Solution for 2hrs at 25C (or overnight at 4C) on a shaker. Again, it is important to make sure the solution covers the entire membrane's surface.

Primary Antibody (50mL)

- 1) 50mL Blocking Buffer
- 2) Primary Antibody (1:1000 for dsRed Polyclonal (mCherry), 1:500 for β – Actin)
- 3) 0.5mL 10% Sodium Azide

The blot is then washed 3 times, 5 mins each wash, with 50mL 1x Rinse Buffer and exposed to a Secondary Antibody Solution for 1hr at 25C (or overnight at 4C) on a shaker; making sure there is enough to cover the membrane's surface.

Secondary Antibody (50mL)

- 1) 50mL Blocking Buffer
- 2) Secondary Antibody (1:20k for Goat Anti-Rabbit HRP-conjugated)

The blot is then again washed 3 times, 5 mins each wash, with 50mL 1x Rinse Buffer. The blot is then exposed to a Western Chemiluminescent HRP Substrate (Immobilon, Millipore) for 5 mins. The blots are then drained of excess substrate and exposed to GenScript Corp High-Sensitivity X-Ray film for 15-45 secs and developed using standard film developing techniques.

Once an image has been obtained for the signal of the chemiluminescent reaction, the intensity of this signal must be processed and quantified. To do so, the images were analyzed using ImageJ Software (Open Source, Public Domain). Measurements were taken of the background and then the intensity of the bands of interest were measured. The corrected intensity was found by subtracting signal from background. This was repeated for both dsRed Polyclonal (detects mCherry domain of PV-mCherry) and β -Actin (ubiquitously expressed cytoskeletal filament protein) antibodies. The intensity of dsRed Poly relative to β -Actin was then used to determine relative expression levels (β -Actin serves as our loading standard and should be constant in each cell regardless of expression of transgene).

In other cases, total protein concentration was used as a loading standard which was performed by a Coomassie Plus Bradford Assay Reagent (Thermo Scientific, Rockford, Illinois) according to manufacturer protocol. In this case, 1 μ L of protein sample is added to 9 μ L dH₂O and added to 300 μ L Coomassie Plus Bradford Reagent, allowed 10mins to react and absorbance measured at 595nm. This absorbance was then subtracted by a “blank” absorbance of 1 μ L Eukaryotic Lysis Buffer with 9 μ L dH₂O and 300 μ L Coomassie Plus Bradford Reagent (contained no protein). The ratio of the signal of dsRed Poly in the Western Blots to the total protein concentration was then used to determine relative expression levels of PV-mCherry transgene.

2.8 – Dynamic Light Scattering

DLS is a commonly used technique that is employed to determine the size of particles in solution. For the purposes of this study, DLS was used to investigate not only the size of the L-QD complexes themselves but whether L-QDs, when mixed with DNA, behaved similarly to cationic liposomes that did not contain QDs.

L-QDs were first diluted to 1 μ g/ μ L in 10mM NaCl, 10mM Tris – HCl pH 7.5 buffer and mixed into 0.5mL eppendorf tubes with PV-mC Plasmid DNA (1 μ g) at various concentration ratios (ranging from 1:1 to 15:1) and allowed 30 mins to complex. Solutions were then placed into a clean, dust free DLS cuvette and analyzed on a Protein Solutions DynaPro Dynamic Light Scattering System with Temperature Controlled Microsampler (Wyatt Technologies Corporation, Santa Barbara, CA) according to manufacturer protocol using 20 sec acquisition time, 5 acquisitions per measurement and 5 measurements per sample. Mean DLS values and Standard Deviations for Particle Diameter are reported.

2.9 – Wide Field Fluorescence Microscopy

The ability to observe transfection events is paramount in the success of this project. Providing a convenient method of observation of this transfection is the basis of the rationale for cloning mCherry onto the C-terminus of Parvalbumin, thus providing the ability to observe transfected cells by fluorescence alone. Wide Field Fluorescence

Microscopy not only allows us to observe which cells are transfected by observing PV-mCherry but also allows us to observe the localization of QDs within these monolayers. Therefore, the use of this technique is crucial in determining the efficacy of L-QDs in the delivery of DNA into CHO cells.

Preparing cells for microscopy is very similar to the preparation of cells described earlier with the exception that trays used for this application are specially designed for optical observation. 3×10^5 CHO cells were plated out as previously described into 10cm^2 optical trays in AB/AM – free media 24 hrs prior to transfection. DNA ($4\mu\text{g}$) is complexed with transfection reagents (either Optifect or L-QDs) and added to culture. Media is changed 6 hrs post-transfection and imaged 48 hrs later on Nikon TE2000-E2 Eclipse microscope (Nikon Instruments Inc., Melville, NY, USA), imaged with a CoolSNAP HQ2 monochrome camera (Photometrics), and analyzed with Nikon NIS Elements software. The cell samples were visualized using a CFI Plan Apochromat 40X objective (NA 0.95, 0.12 mm WD) equipped with differential image contrast (DIC). Wide field microscopy utilized an X-Cite TM 120 power supply and FITC and TRITC filter cubes (31000 series standard filter sets, Chroma technologies).

2.10 – Cryo Electron Microscopy

In previous studies, it was observed that when organic phase QDs were incorporated into cationic liposomes, no evidence of any QD was observed in the liposome's internal aqueous environment as seen by Cryo-EM. Yet, these samples are fluorescent and successfully deliver QDs into cells both in vitro and in vivo. It was then ascertained that they were encapsulated into the alkyl environment of the liposome's bilayer as evidenced by small dark imperfections in the liposome's membrane. For this study, it was of interest to know whether the same characteristics would be observed in the L-QD formulations prepared as previously described.

Samples were prepared by first diluting 4mg/mL L-QDs in dH_2O to 1mg/mL with dH_2O . Afterward, $2\mu\text{L}$ of this solution is then placed onto Quantifoil R 2/1 grids (Quantifoil Micro Tools GmbH, Jena, Germany) and frozen using a Vitrobot Mark IV Automated Vitrification Device (FEI, Hillsboro, Oregon) with blot times varying from 2 to 3 seconds, 100% humidity and plunged into liquid-phase ethane. Vitrified samples were

then placed into liquid nitrogen then imaged on a FEI CM 120 TEM microscope (FEI, Hillsboro, Oregon) with Tungsten filament and a Phillips CryoEM Anticontaminator.

2.11 – Flow Cytometry

In addition to knowing the amount of protein produced in a given cell population, it is also of significant value to be able to quantify what percentage of cells are producing the protein of interest following a transfection event. Flow Cytometry provides a method to quantify percentages of transfected cells based on the fluorescence exhibited by cells expressing the PV-mCherry fusion peptide.

Cells intended for the use of Flow Cytometry are prepared identically to those prepared for standard transfection procedure. 3×10^5 cells in a 10cm^2 dish are transfected as described previously. 48 hrs following transfection, cells are washed 1x with TBS and trypsinized by TLE. Cells are then suspended into 1mL complete media and placed into a 15mL Falcon Tube. Cell suspension is then centrifuged at 800rpm for 10mins. Following centrifugation, the supernatant is removed (as much as possible without disrupting the pellet) and re-suspended in 1mL Hank's Balanced Salt Medium and placed on ice.

Cells are then run through a BD FACS Canto II with 488 nm excitation and detection on FITC (530/15) and PE-A (585/42) filter sets.

CHAPTER 3: RESULTS AND DISCUSSION

3.1 – Cloning and Expression of PV-mCherry Fusion Protein

The initial step in the cloning process, as mentioned earlier, was to clone the PV gene onto the N-terminus of mCherry in plasmid pmCherry N-1 (Clontech). Parvalbumin Major Isoform I taken from *D. sabina* was obtained from Dr. Moerland and the initial PCR was performed. Afterward, agarose gel electrophoresis was used to characterize the resulting product. What was observed was a band of approximately 370bp, indicating a successful PCR of the desired gene (**Figure 3.1**).

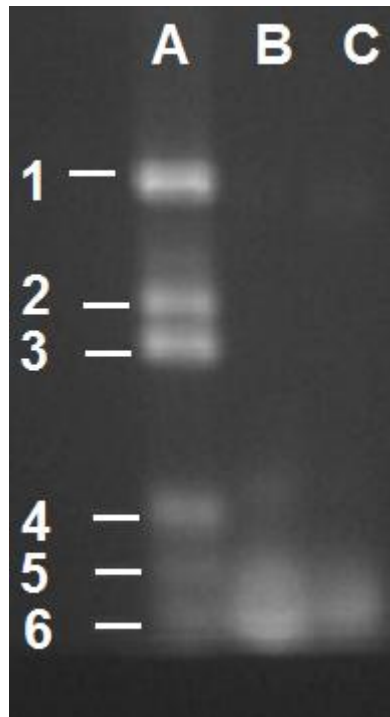


Figure 3.1: Agarose Gel of PCR products of PV insertion into pmCherry N-1. Lane A is pGem DNA ladder (FSU Cloning Facility); band from lane A are: **1**) 2977bp **2**) 1799bp **3**) 1508bp **4**) 724bp **5**) 517bp **6**) 396bp. Lanes B and C are PCR products from PV insert. The bands in lanes B and C are those corresponding to the approximately 370bp PCR products of Parvalbumin with additional base pairs from the primers used in the PCR reaction.

This PCR product was then purified and it, along with the pmCherry N-1 plasmid, were cleaved with Xho I and BamH I enzymes. Agarose gel electrophoresis was then used to confirm the cleavage of the pmCherry N-1 plasmid and showed successful cleavage for both enzymes (**Figure 3.2**).



Figure 3.2: Agarose Gel of pmCherry N-1 Plasmid cleavage by Xho I, BamH I and both respectively. **Lanes 1)** pGem DNA ladder (FSU Cloning Facility) **2)** Uncut pmCherry N-1 **3)** Xho I cleaved pmCherry N-1 **4)** BamH I cleaved pmCherry N-1 **5)** double digested pmCherry N-1

After confirmation of the success of the double digestion of Xho I and BamH I on the plasmid DNA, it was now known that the ends of the plasmid were complimentary to the ends of the cleaved PCR insert. Therefore a ligation was then performed. Following

transformation into a bacterial cell line, growth and purification, the resulting plasmid was then submitted for sequencing. Sequence analysis then confirmed the successful insertion of PV onto the N-terminus of mCherry.

Following sequence analysis and confirmation of successful cloning, Site-Directed Mutagenesis was then performed to remove the internal Kozak sequence that lies between PV and mCherry as discussed earlier. Sequence analysis confirmed the successful mutation of the internal Kozak (**Figure 3.3**). This CMV-promoter PV-mCherry plasmid was then complete and available for expression tests in CHO cells.

ACGGTAAACTGCCCACTTGGCAGTACATCAAGTGTATCATATGCCAAGTACGCC
 CCTATTGACGTCAATGACGGTAAATGGCCGCCTGGCATTATGCCAGTACATGAC
 CTTATGGGACTTTCCTACTTGGCAGTACATCTACGTATTAGTCATCGCTATTACCAT
 GGTGATGCGGTTTTGGCAGTACATCAATGGGCGTGGATAGCGGTTTACTCACGG
 GGATTTCCAAGTCTCCACCCCATTGACGTCAATGGGAGTTTGTGTTTGGCACCAA
 ATCAACGGGACTTTCAAAATGTCGTAACAACCTCCGCCCATGACGCAAATGGG
 CGGTAGGCGTGTACGGTGGGAGGTCTATATAAGCAGAGCTGGTTTAGTGAACCGT
 CAGATCCGCTAGCGCTACCGGACTCAGATCTCGAGCTCCTGCAAGTCGACGGTCCG
 CCACCATGGATATTACAGATGTGCTTGCCAAGGATGACATTAATAAAAGCCCTGGA
 CAATTTCCAAAAGCCCGGAAGCTTCAATCACAAGGTGTTCTTCGACATGGTTGGT
 TTGAAGAAGAAGGCGAAGACTGATGTGGAGAAAGTCTTCAAATCCTCGACAAG
 GATCAGAGTGGCTACATTGAAGAGGATGAGCTGAAACATATACTACAGTGTGTTTGC
 ACCCAATGGAAGAGATCTTGCCGATAACGAAATTCAGGCACTTCTCGCAGCCGGT
 GATGAGGATCATGATGGCAAGATTGGGCAGTCAGAGTTTGTCAACCTCGTAGGTC
 AAGCAAGCCCGGGATCCACCGGTCGCGGCCATGGTGAGCAAGGGCGAGGAGGAT
 AACATGGCCATCATCAAGGAGTTCATGCGCTTCAAGGTGCACATGGAGGGCTCC
 GTGAACGGCCACGAGTTCGAGATCGAGGGCGAGGGCGAGGGCCGCCCTACGA
 GGGCACCCAGACCGCCAAGCTGAAGGTGACCAAGGGTGGCCCCCTGCCCTTCG
 CCTGGGACATCCTGTCCCCTCAGTTCATGTACGGCTCCAAGGCCTACGTGAAGCA
 CCCCGCCGACATCCCGACTACTTGAAGCTGTCCTTCCCCGAGGGCTTCAAGTG
 GGAGCGCGTGATGAACCTTCGAGGACGGCGGCGTGGTGACCGTGACCCAGGACT
 CCTCCCTGCAGGACGGCGAGTTCATCTACAAGGTGAAGCTGCGCGGCACCAACT
 TCCCCTCCGACGGCCCCGTAATGCAGAAGAAGACCATGGGCTGGGAGGCCTCCT
 CCGAGCGGATGTACCCCGAGGACGGCGCCCTGAAGGGCGAGATCAAGCAGAGG
 CTGAAGCTGAAGGACGGCGGCCACTACGACGCTGAGGTCAAGACCACCTACAA
 GGCCAAGAAGCCCGTGCAGCTGCCCGGCGCCTACAACGTCAACATCAAGTTGGA
 CATCACCTCCACAACGAGGACTACACCATCGTGGAACAGTACGAACGCGCCGA
 GGGCCGCCACTCCACCGGCGGCATGGACGAGCTGTACAAGTAG

Red = mCherry Red Fluorescent Protein
 Yellow = Parvalbumin Major Isoform
 Light Blue = Sal I Restriction Site
 Dark Blue = Spacer
 Green = Functional Kozak Sequence
 Magenta = CMV promoter
 Black = Xho I Restriction Site
 Purple = Mutated, Non-Functional Kozak Sequence
Peach = Non-coding spacer DNA

Figure 3.3: Results of sequence analysis for PV-mCherry Fusion Plasmid

Since the PV-mCherry fusion gene had been successfully sequenced and the internal Kozak sequence removed, it was then important to investigate whether this gene

expressed in mammalian cells. CHO cells were transfected with PV-mCherry (CMV promoter) using Optifect Commercial Transfection Reagent and analyzed by Western Blot (**Figure 3.4**) and Wide-Field Fluorescence Microscopy (**Figure 3.5**).

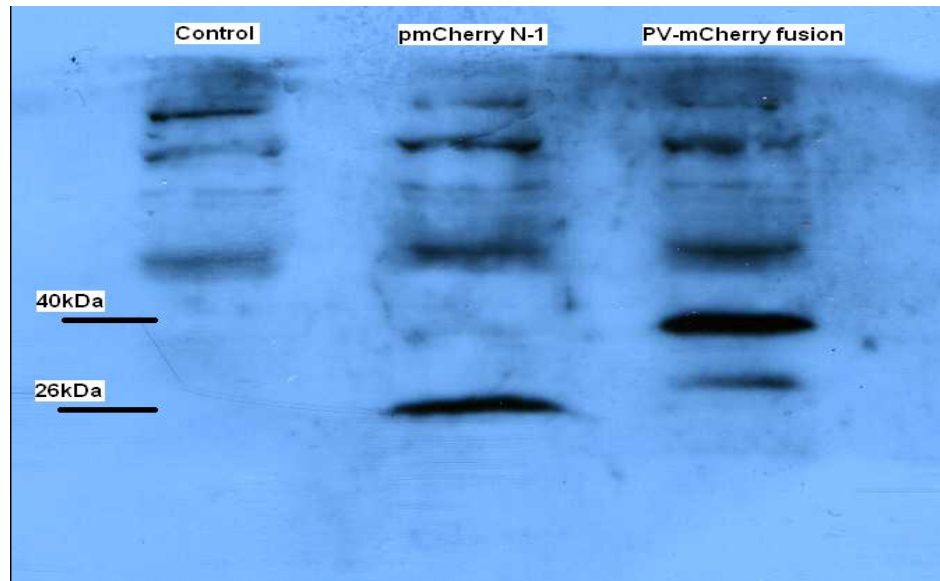


Figure 3.4: Western of CHO with PV-mCherry using Optifect Commercial Transfection Reagent. This has been blotted against dsRed Polyclonal primary antibody. Three samples were run. The left lane is CHO cells transfected with Optifect but no plasmid (Control). The middle lane is CHO cells transfected with un-cloned pmCherry N-1 plasmid with Optifect. The right lane is CHO cells transfected with cloned PV-mCherry fusion plasmid with Optifect.

This western blot has several bands in each lane, most of which is non-specific interaction between the dsRed Polyclonal Primary antibody and the proteins contained in the CHO lysate. This is seen in each lane, including lane 1 which received no plasmid whatsoever. The band of interest are those that are observed in lanes 2 and 3 which are not present in lane 1. The dark band at the bottom of lane 2 is that of the mCherry protein expressed from an unmodified commercial pmCherry N-1 plasmid. The size of the mCherry protein itself is approximately 26kDa. In lane 3 two dark bands are observed that are not present in either lanes 1 or 2. The top band, which is also the more intense of the two, corresponds to the PV-mCherry protein. The size of PV is

approximately 13kDa and the size of mCherry 26kDa, therefore the combined size of the fusion peptide is roughly 40kDa (taking into account a 27bp spacer sequence corresponding to 9 amino acids). The smaller and less intense band was not expected. It is obviously larger than that of unmodified mCherry but significantly smaller than that of the PV-mCherry fusion. This is most likely the product of some sort of proteolytic cleavage event that occurs after the translation of the finished PV-mCherry product. It is possible that within the spacer sequence there exists a protease cleavage site that removes the PV from the mCherry protein but leaves much of the spacer intact, therefore creating a protein that is slightly larger than the mCherry peptide.

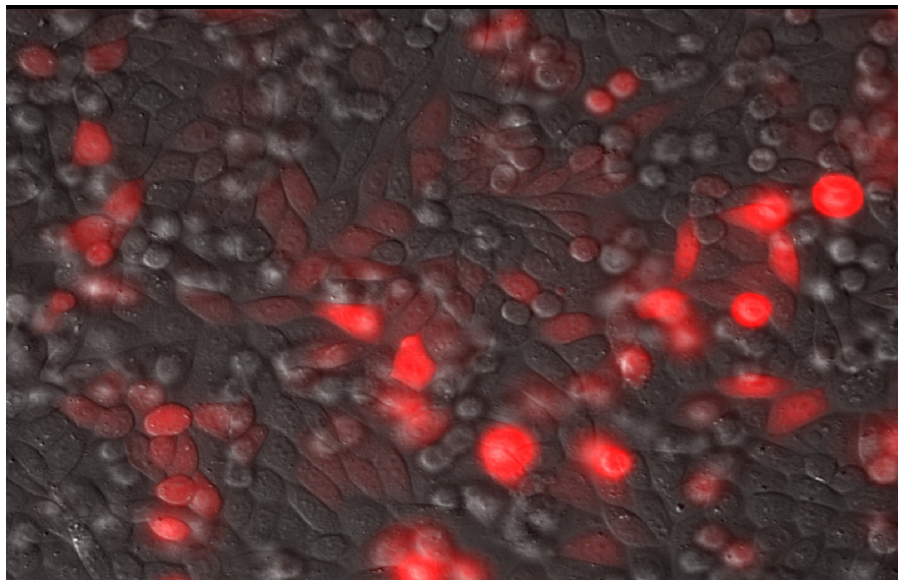


Figure 3.5: Wide-field fluorescence microscopy image of CHO cells transfected with PV-mCherry. Cells that are red are those that are expressing mCherry protein. This demonstrates the functionality of the plasmid and that the fusion of PV onto the mCherry protein does not interfere with the folding of the mCherry protein in any way that compromises its fluorescence.

This image was taken using an excitation laser of 512nm and captured using an TRITC filter cube as described earlier. As is evident from the image, many cells are emitting red, which is indicative of cells expressing PV-mCherry protein. The peak excitation and emission wavelengths of mCherry are 585 and 610nm, respectively.

Therefore, if a laser with a larger (redder) excitation wavelength were used, it would be possible to observe a much higher level of emission from these cells with reduced background; potentially revealing many cells that are expressing mCherry but are not able to be observed under these conditions. Nevertheless, this image lends credibility to the information obtained from the Western Blots. It shows that indeed CHO cells transfected with the PV-mCherry fusion plasmid express a fully functional fluorescent protein *in vitro*.

It was then evident that the PV-mCherry (CMV promoter) plasmid was successfully cloned, able to be expressed in CHO cells and the resulting protein functional. The next step, as described previously, was to sub-clone this fusion construct into the α -MyHC plasmid. As mentioned previously, this was done by first removing the Hind III cut site from within the PV-mCherry fusion construct by Site-Directed Mutagenesis followed by PCR and insertion into a the plasmid. Following SDM, a PCR of the PV-mCherry fusion insert was performed and characterized by agarose gel electrophoresis (**Figure 3.6**).

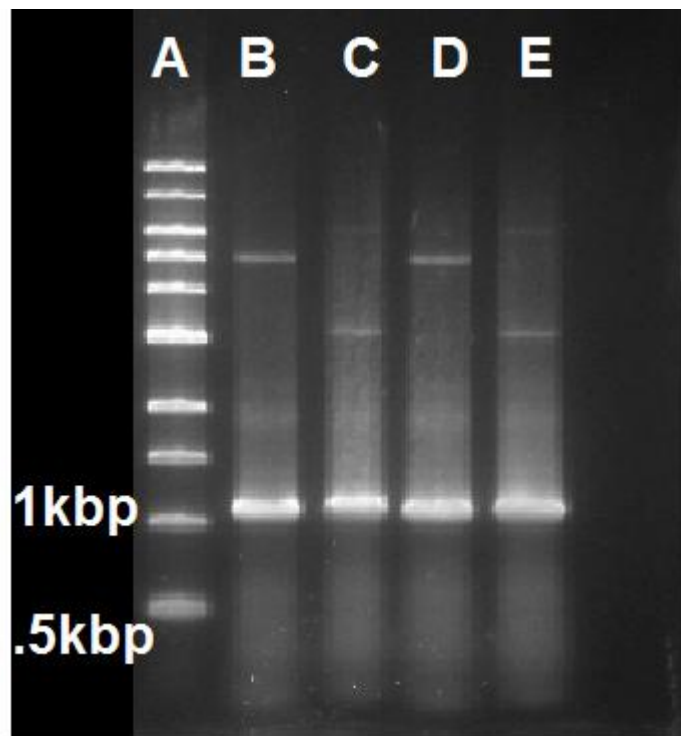


Figure 3.6: Agarose Gel of PCR products of PV-mCherry inserts into α -MyHC. **Lanes:** **A)** 1kbp DNA ladder, **B** and **D)** Double Digests of PCR products with Sal I and Hind III, **C** and **E)** Undigested PCR products. The first two bands of the 1kbp DNA ladder correspond to 500 and 1000 bp, respectively.

The agarose gel of this PCR reaction and the subsequent cleavage show that the PCR reactions created a product that is significantly larger than that of 1000 bps. The PCR product expected from this reaction is approximately 1300bp (PV is ~ 300bp, mCherry is ~ 1000bp). Furthermore, those products shown in lanes B and D are slightly smaller than those shown in lanes C and E. Seeing as these are the double digests of the PCR products with Sal I and Hind III, it is logical to conclude that this is the result of the ends being cleaved off by the restriction enzymes mentioned previously. Also worth mentioning is that when the PCR products of this reaction are digested by these two restriction endonucleases, they produce single bands. This indicates the SDM to remove the internal cut site of Hind III within the PV-mCherry fusion peptide was successful. If it were not and the Hind III cut site remained, we should observe two bands but that is not observed in this gel. Therefore, based on the results of this gel

both SDM, PCR of the desired gene sequence and the subsequent cleavage by Sal I and Hind III were successful. Afterward, the sub-cloning into α -MyHC was performed as described earlier and the resulting plasmid's sequence analyzed (**Figure 3.7**).

CTCTGCCAGCTGCCGGCACTCTTAGCAAACCTCAGGCACCCTTACCCACATAGACCTCTGA
 CAGAGAAGCAGGCACCTTACATGGAGTCCTGGTGGGAGAGCCATAGGCTACGGTGTGA
 AAAGAGGCAGGGAAGTGGTGGTGTAGGAAAGTCAGGACTTCACATAGAAGCCTAG
 CCCACACCAGAAATGACAGACAGATCCCTCCTATCTCCCCATAAGAGTTTGAGTC
GACGGT**C****GCCACCATGG**ATATTACAGATGTGCTTGCCAAGGATGACATTA
 AAAAAAGCCTGGACAATTTCCAAAAGCCCGGGAGCTTCATCACAAGGTGTTCTTCGACATGGT
 TGGTTTGAAGAAGAAGGCGAAGACTGATGTGGAGAAAGTCTTCAAATCCTCGACA
 AGGATCAGAGTGGCTACATTGAAGAGGATGAGCTGAAACATATACTACAGTGT
 TTTG CACCCAATGGAAGAGATCTTGCCGATAACGAAATTCAGGCACCTTCTCGCAGCCGGT
 GATGAGGATCATGATGGCAAGATTGGGCAGTCAGAGTTTGTCAACCTCGTAGGTCA
 AGCAG**CCCGGGATCCACCGGTCGCGGCCATGGT**GAGCAAGGGCGAGGAGGATAA
 CATGGCCATCATCAAGGAGTTCATGCGCTTCAAGGTGCACATGGAGGGCTCCGTGA
 ACGGCCACGAGTTCGAGATCGAGGGCGAGGGCGAGGGCCGCCCTACGAGGGC
 ACCCAGACCGCCAAGCTGAAGGTGACCAAGGGTGGCCCCCTGCCCTTCGCCTGG
 GACATCCTGTCCCCTCAGTTCATGTACGGCTCCAAGGCCTACGTGAAGCACCCCGC
 CGACATCCCCGACTACTTGAAGCTGTCTTCCCCGAGGGCTTCAAGTGGGAGCGC
 GTGATGAACTTCGAGGACGGCGGCGTGGTGACCGTGACCCAGGACTCCTCCCTG
 CAGGACGGCGAGTTCATCTACAAGGTGAAGCTGCGCGGCACCAACTTCCCCTCCG
 ACGGCCCGTAATGCAGAAGAAGACCATGGGCTGGGAGGCCTCCTCCGAGCGGAT
 GTACCCCGAGGACGGCGCCCTGAAGGGCGAGATCAAGCAGAGGCTGAAGCTGAA
 GGACGGCGGCCACTACGACGCTGAGGTCAAGACCACCTACAAGGCCAAGAAGCC
 CGTGACGCTGCCCGGCGCCTACAACGTCAACATCAAGTTGGACATCACCTCCAC
 AACGAGGACTACCCATCGTGAACAGTACGAACGCGCCGAGGGCCGCCACTCCA
 CCGGCGGCATGGACGAGCTGTACAAGTAG**CGGAAGCTT**GATGGGTGGCATCCCTG
 TGACCCCTCCCAGTGCCCTCCTGGCCCTGGAAGTTGCCACTCCAGTGCCACC
 AGCCTTGTCTAATAAAATTA

Blue = Sal I Cut Site

Dark Blue = Linker Between Parvalbumin and mCherry

Green = Functional Kozak Sequence

Yellow = Parvalbumin Major Isoform I Gene (*D. sabina*)

Purple = Mutated, non-functional Kozak Sequence

Brown = Alpha Myosin Heavy Chain promoter (as reported in GenBank # u71441)

Red = mCherry Red Fluorescent Protein Gene (Clontech)

Grey = Mutated Hind III Cut Site within Parvalbumin Major Isoform I

Violet = Functional Hind III Cut Site

Peach = Spacers

Figure 3.7: Sequence of α -MyHC PV-mCherry fusion plasmid. This sequence analysis confirms the perfect cloning of PV-mCherry fusion peptide, the removal of the internal kozak on the N-terminus of mCherry, the removal of the Hind III cut site within Parvalbumin and the successful insertion of this entire construct into the α -MyHC promoter plasmid.

The results of this sequence analysis confirm that the PV-mCherry insert was successfully sub-cloned into the α -MyHC plasmid in the correct orientation and the promoter elements of the α -MyHC plasmid are of the correct sequence. The sequence shows that there were no errors in the PCR reaction, creating a product of identical code to that of the original copy. Also indicated in the code is the successful removal of the internal Hind III cut site of the PV-mCherry insert. Therefore it can be concluded that the entirety of cloning for this project has been successfully completed.

Next, it was necessary to test the discriminatory expression of the successfully cloned α -MyHC PV-mCherry plasmid. This was done by Flow Cytometry. CHO cells were transfected with Optifect only (no plasmid), the CMV PV-mCherry and α -MyHC PV-mCherry plasmids; using Optifect in both instances (**Figure 3.8**).

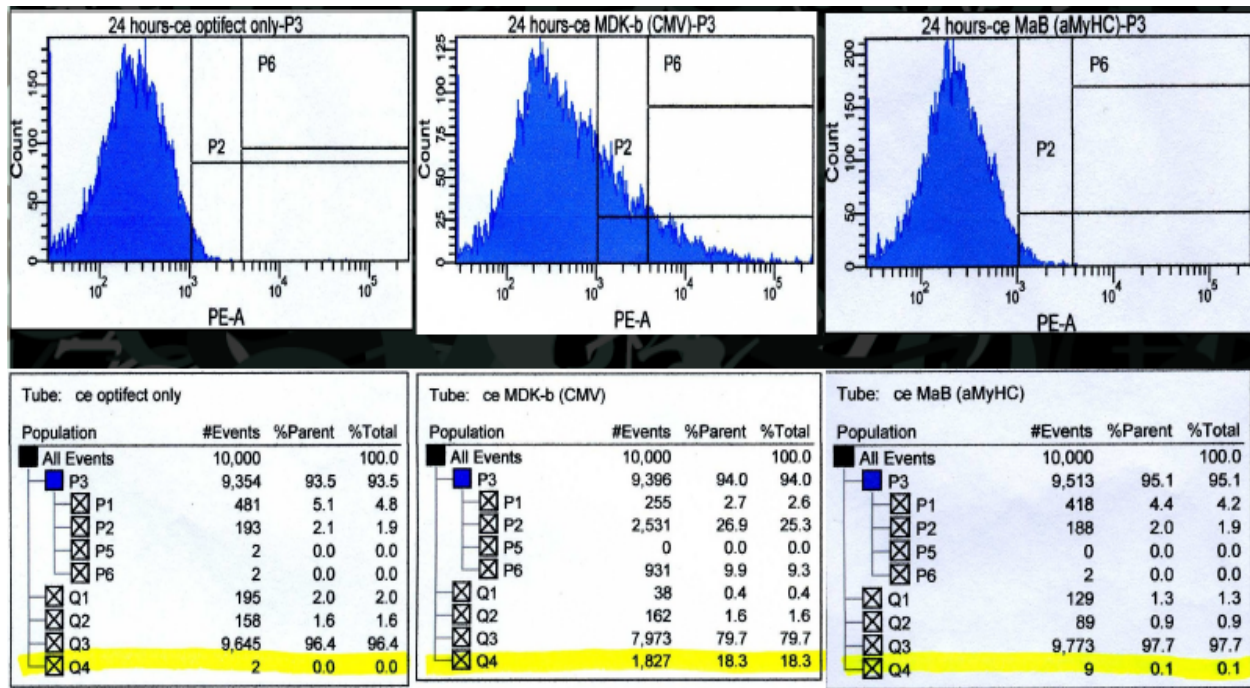


Figure 3.8: Results of Flow Cytometry of CHO cells transfected with CMV and α -MyHC PV-mCherry. The charts on top illustrate the number of events versus the level of fluorescence observed using a PE-A filter set (note x-axis is log-scale). The information on the bottom shows the number and percentage of events that break certain threshold values of PE-A, indicating red fluorescent cells (transfected cells, highlighted in yellow). The left are those cells transfected with Optifect only. Which show 0.0% fluorescence, indicating no transfection event. The middle are those cells transfected with CMV PV-mCherry, which show approximately 18.3% fluorescence. The right are those cells transfected with α -MyHC PV-mCherry, which show 0.1% fluorescence.

The results of Flow Cytometry show that while CMV PV-mCherry expresses in CHO cells, as expected and already confirmed, the α -MyHC PV-mCherry does not. While this does not confirm the functionality of the α -MyHC plasmid in cardiac cells, it does show that this plasmid does not express in CHO cells. However, based on sequence analysis results, it is reasonable to presume that this plasmid would express in cardiac tissue. It is also worth noting that a 488nm excitation laser was utilized in this experiment, which again, as before, provides only a minimum of excitation for mCherry. Therefore, although we only see a 18.3% transfection rate for CMV PV-mCherry in this experiment, it is highly likely that a much higher percentage of these cells are actually

expressing mCherry but only the most robust of these cells are being identified by the detector.

This information is highly important to the utility of these technologies as it is important to be able to target the expression of a protein to a specific cell type. By coupling cell-specific promoters with targeting peptides or antibodies, it would then be feasible to design an efficient delivery system that would be almost entirely devoid of random expression in undesired cell types, thus facilitating the delivery of gene therapeutics without the consequences or side effects of aberrant transfection.

3.2 – Synthesis of CdSe/ZnS and Encapsulation into Liposomes

Synthesis of core CdSe and subsequent ZnS capping was performed as described earlier. Afterward, absorption and emission spectra obtained from the synthesized products (**Figure 3.9** and **Figure 3.10**, respectively). Peak absorption and emission was observed at around 525nm and 550nm, respectively.

As described earlier, QDs were cleaned by dilution in toluene and precipitation by methanol, dried and combined with lipids in chloroform. The lipid and QD solution was then sonicated and dried under N₂ stream. The film was reconstituted in dH₂O and sonicated until clear. Emission spectrum was collected from this L-QD solution, which exhibited fluorescence characteristic of the QDs with peak emission around 550nm (**Figure 3.11**). This indicates a successful encapsulation of organic-phase CdSe/ZnS QDs into the liposome's alkyl region.

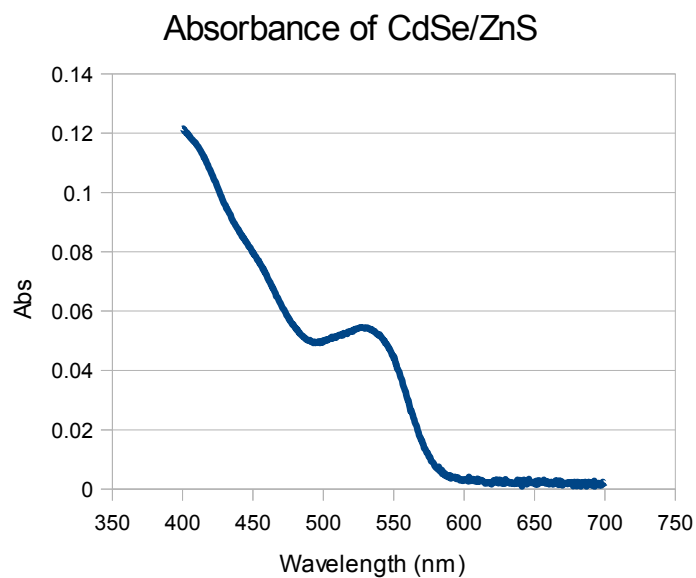


Figure 3.9: Absorption Spectra of CdSe/ZnS in Toluene. This shows a peak absorption around 525nm.

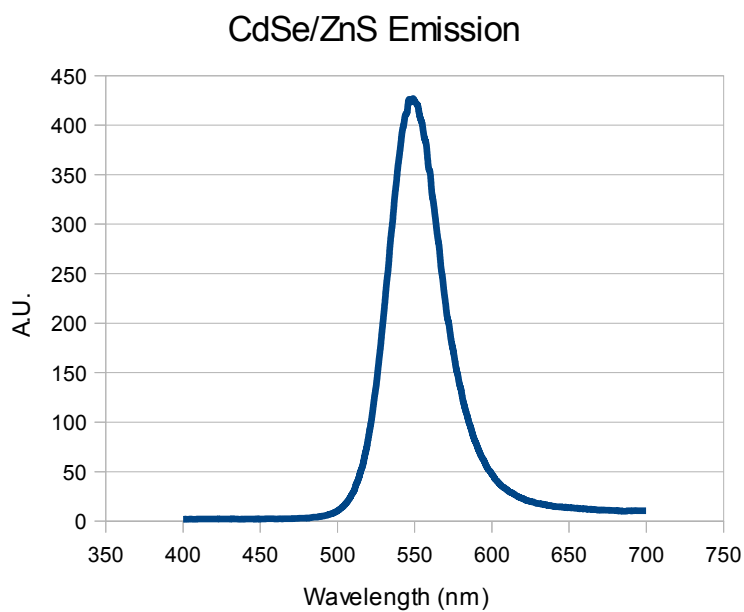


Figure 3.10: Emission spectra of CdSe/ZnS in Toluene. Peak emission is observed around 550nm.

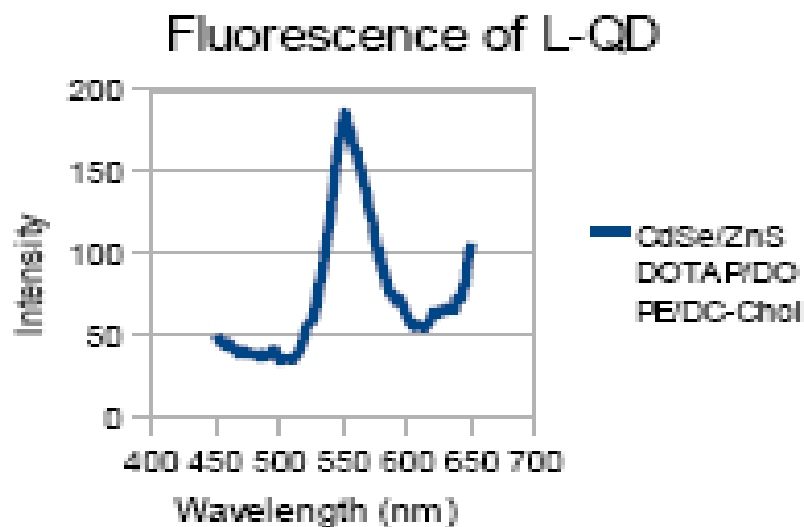


Figure 3.11: Fluorescence spectra of L-QDs in dH₂O. Peak emission is observed around 550nm, identical to that observed with QDs prior to lipid-encapsulation. Also some scattering is observed as the emission approaches 700 which is the result of scattering of the 350nm excitation source. This shows that QDs are solubilized by the liposomes and that they are still emissive in dH₂O.

L-QDs were then diluted in Tris buffer and Cryo-Em was performed as described earlier. Many of the images show unilamellar liposomes of approximately 40nm in diameter (**Figure 3.12**). While no QDs can be observed in these images, it is reasonable to state that a higher resolution would have to be used in order to clearly see something that small in size (approximately 4nm). The hypothesis of Kostarelos et al is that the organic phase QDs become entrapped into the alkyl region of the liposomes lipid bilayer, thus stabilizing them in the organic environment and for the most part protecting them from the outside aqueous environment. While this phenomenon is not able to be clearly observed by these images, this solution remained fluorescent, indicating that the lipids have somehow made the QDs soluble in this aqueous phase. This is most likely some kind of association with the hydrophobic region of the bilayer.

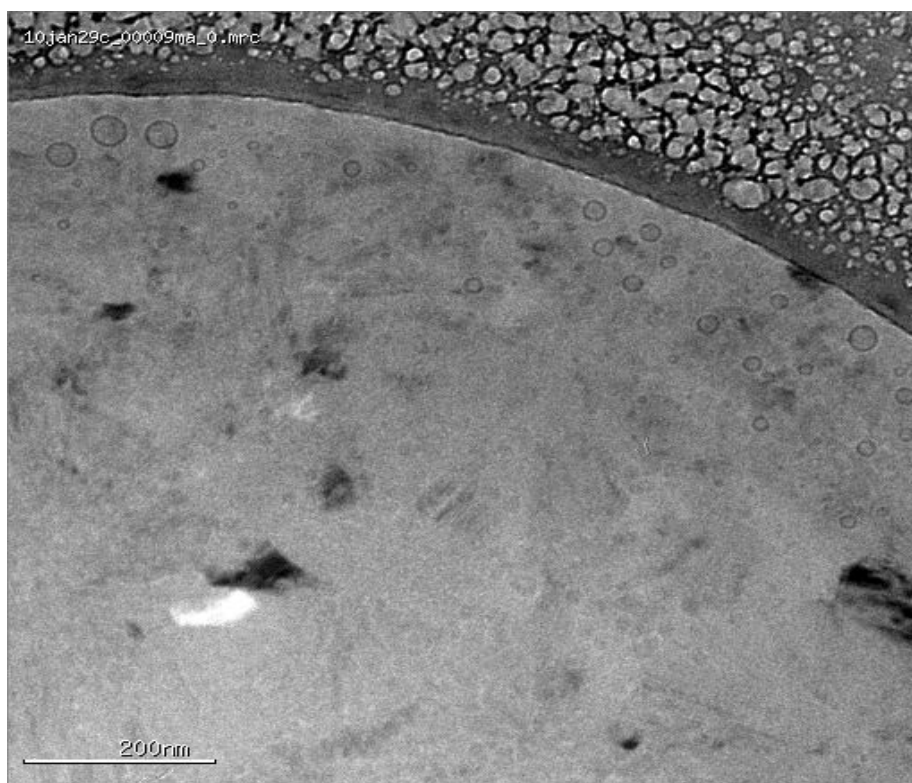


Figure 3.12: Cryo-EM Image of L-QDs. This image shows the presence of liposomes ranging in size from approximately 40 nm in diameter.

3.3 – Internalization of L-QDs, Association and Delivery of DNA into CHO Cells

Following the successful incorporation of QDs into liposomes, it was then necessary to investigate the L-QDs ability to be internalized into cells and observed. This was done by performing a procedure that was a slight modification of transfection protocol described previously. L-QDs (1:1 DOTAP:DOPE molar lipid composition) were added to CHO cells that had been seeded in optical trays and allowed 6hrs and then cells were washed and given fresh media. Cells were then imaged by Fluorescence Microscopy (**Figure 3.13**). The image shows that there is a significant presence of L-QDs in and around CHO cells. This image was taken 48hrs after the addition of these L-QD hybrids to the cell cultures, showing substantial stability in the intracellular as well as extracellular environment. This is in agreement with observations made previously by Kostarelos et al. Having been successful in this initial trial, it was then determined that it

was reasonable to continue studies investigating the association of these L-QDs with DNA and their ability to deliver said DNA into CHO cells for transfection.

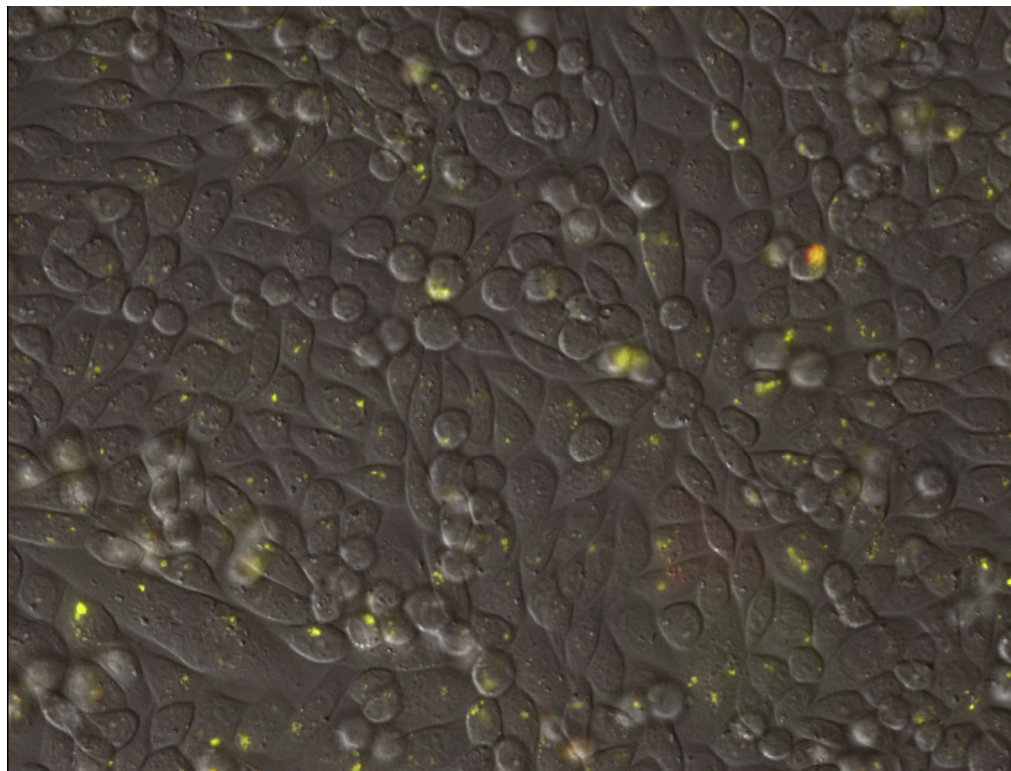
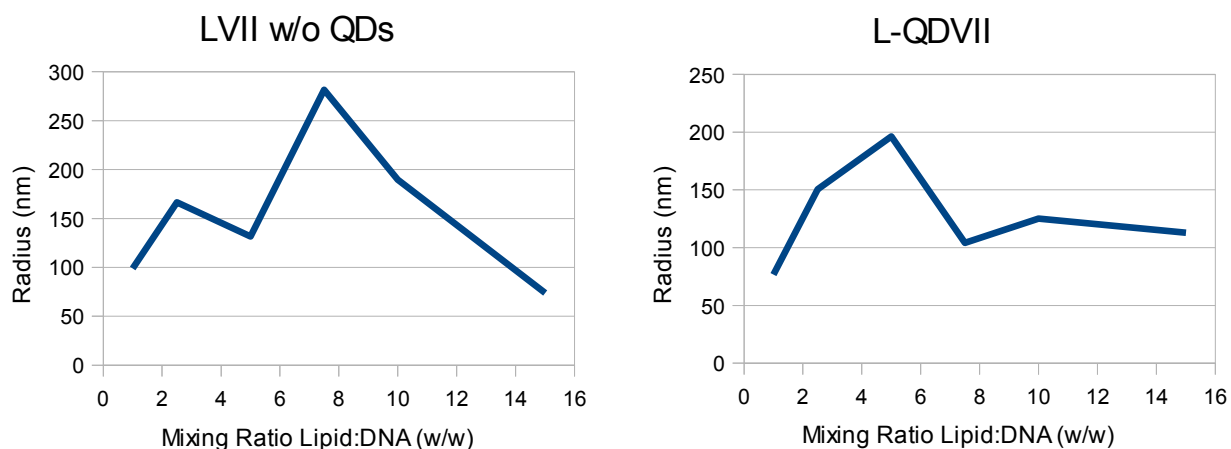


Figure 3.13: Wide-Field Fluorescence Microscopy image of CHO cells with L-QD VII. Punctate yellow dots are the emission of the CdSe/ZnS QDs within the cell.

The association of L-QDs with DNA was observed through the technique of Dynamic Light Scattering. As discussed earlier in the work by Sakurai et al, the association of lipids with DNA at various mixing ratios results in differences in the sizes and transfection efficiency of the complexes. Therefore it was the goal of this procedure to attempt to observe any changes in the sizes of the complexes that result from changes in the mixing ratio of L-QD to DNA and to compare that to those liposomes that do not contain any QDs (**Figure 3.14**).

The results of this study show that there is indeed a correlation between the mixing ratio of L-QD:DNA and the size of the complexes. Interestingly, those liposomes

that contain QDs appear to behave differently than those that do not contain QDs with regard to complex size. Those liposomes that contain QDs appear to reach a maximum in size at a mixing ratio of 5:1 (Lipids:DNA w/w) while those that did not contain QDs reach a maximum in size at around 7.5:1. This is contrary to the findings of Sakurai et al, which found a ratio of 5:1 to yeild the largest complexes but still shows that a maximum is reached, after which point the complexes become significantly smaller upon the further addition of cationic lipids. This data illustrates the general tendency observed by Sakurai et al, leading one to assume this is due to the association of the liposomes with the plasmid DNA. What is odd however is that there



<u>Complex and Mixing Ratio</u>	<u>Radius</u>	<u>Standard Deviation</u>	<u>% Polydispersity</u>
LVII w/o QDs Only	80.25	3.31	67.8
1	98.89	14.5	75.9
2.5	166.57	18.7	78.4
5	131.7	6.7	38.6
7.5	281.53	24.6	73.9
10	189.56	20.5	91.1
15	73.7	3.6	54.7
LQDVII Only	90.58	4.86	65.4
1	76.7	29.45	109.8
2.5	150.66	34.3	84.6
5	196.3	12	64.7
7.5	104.18	9.7	62.7
10	125.26	8.8	68.1
15	112.98	3.8	56.5

Figure 3.14: Results of Dynamic Light Scattering of LVII and LQDVII. *Top Left:* Radius as a function of mixing ratio for Liposomes w/o QDs. *Top Right:* Radius as a function of mixing ratio for Liposomes with QDs. Bottom: Tabulated results listing average radius, standard deviation between measurements and polydispersity of complexes.

appears to be a disparity in the information it provides. For example, the size of the L-QD-DNA complex when a single equivalent addition of DNA is added is shown to be less than that of the L-QDs alone. This is also observed when 15 equivalents of Liposomes w/o QDs are added to DNA. Also worth mentioning is the disparity between the data provided by Dynamic Light Scattering and that of Cryo Electron Microscopy regarding the size of the L-QD liposomes. Images taken by Cryo-EM show liposomes of

approximately 40nm while DLS reports liposomes of approximately 160-180nm. Whatever the cause of this disparity, it is evident that as we modify the mixing ratio of L-QDs to DNA, the sizes of these complexes are greatly affected.

Now knowing that our L-QDs are able to be internalized into CHO cells and that they are able to bind DNA in a manner that is similar to that of liposomes of the same constitution that do not contain QDs, it was then of interest to examine whether the L-QD-DNA complexes are able to be internalized and expressed in CHO cells. This was determined by performing Wide Field Fluorescence Microscopy on cells transfected with these L-QD-DNA complexes using a procedure very similar to those described earlier. L-QDs were combined with DNA at a ratio of 5:1 L-QD:DNA and added to CHO cells of approximately 70% confluency. After 6 hrs the media was removed, cells washed and fresh media given. 48Hrs later the cells were imaged (**Figure 3.15**).

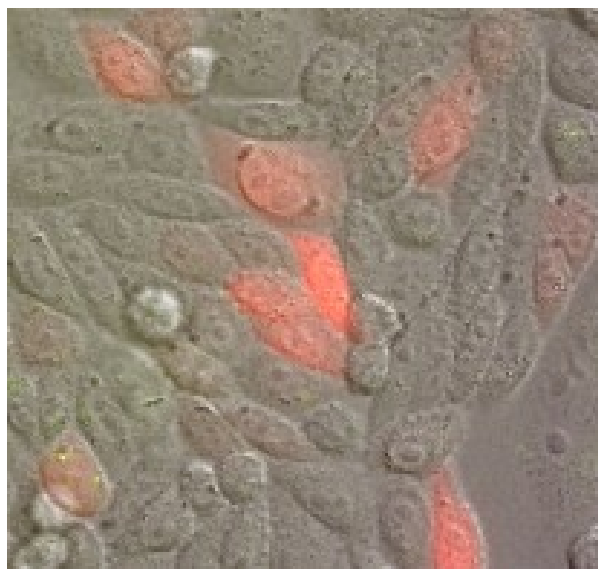


Figure 3.15: Wide-Field Fluorescence Microscopy of CHO with PV-mCherry using LQDVII. This image clearly shows the expression of mCherry in a number of cells. Less obvious is the presence of QDs within these cells (Yellow punctate dots are the emission of CdSe/ZnS).

This image illustrates the ability of the L-QDs to deliver DNA into CHO cells and that this DNA is expressed. Although this image clearly shows the expression of PV-mCherry what is difficult to see is the presence of QDs in these cells. This is due primarily to the laser/filter combination used to detect the QDs. A 488nm excitation laser with a FITC filter was used to observe these QDs. Upon examining the absorption spectrum of the QDs used for these experiments, a trough is present at the wavelength of light used to excite these QDs, therefore very low emission is observed. If a combination of a 512nm laser with a FITC filter were used, a much better image would be observed for the presence of QDs in these cells.

It is now known that L-QDs bind and deliver DNA to CHO cells. It was then logical, keeping in line with the observations of Sakurai et al that the transfection efficiency as well as the size of a liposome-DNA complex is affected by the mixing ratio of lipids to DNA, to test the transfection efficiency of this formulation of lipids as a function of L-QD:DNA mixing ratio. To do so, CHO cells were transfected with L-QD-DNA complexes mixed at ratios ranging from 0.75:1 to 7.5:1 in a manner consistent with previous transfections. The resulting expression was then compared via Western Blot with the expression of commercial reagents and equivalent liposomes without QDs (**Figure 3.16**).

This Western Blot shows that for liposomes of composition 1:1 DOTAP:DOPE the optimal ratio of transfection efficiency in CHO cells is at approximately 5:1. A steady increase in the rates of expression is observed as the ratio of L-QD is increased until 5:1 at which point it declines considerably. It also shows that this formulation of lipids is largely outperformed by commercial reagent Optifect. It should be said however, that although not as efficient as commercial reagent for the expression of transgenes, this was simply the first formulation used, one that is similar in composition to that used by Felgner et al in their initial trials in 1989. This then led to the desire to develop a formulation that would perform at a much higher level of efficacy, perhaps even able to compete and perform on par with commercial formulations.

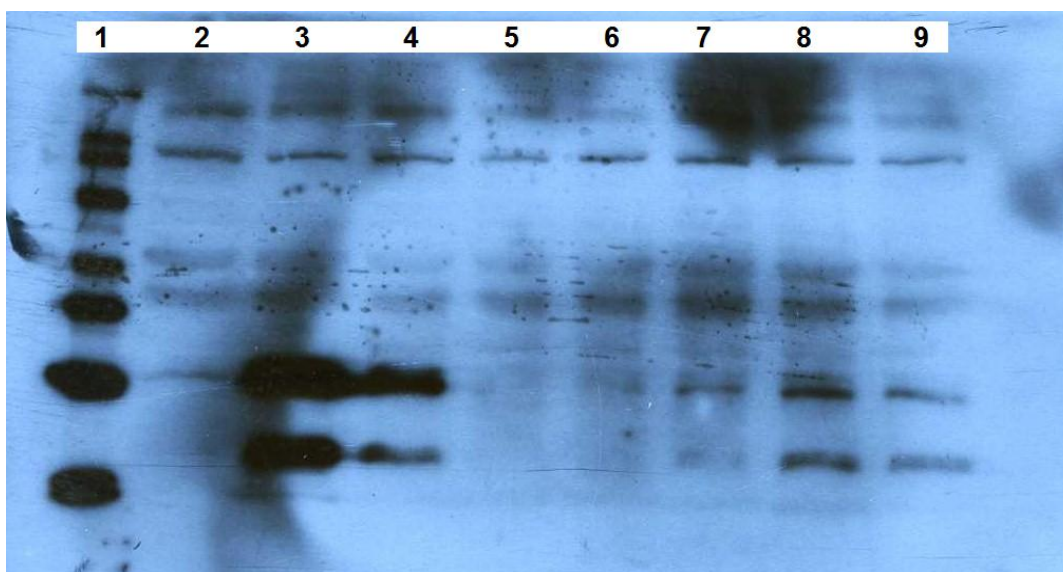


Figure 3.16: Western of CHOs transfected with PV-mCherry plasmid using LQDVII.

Lane 1) Magic Mark Size Marker

Lane 2) Negative Control. Received no transfection reagent.

Lane 3) Optifect Commercial Transfection Reagent.

Lane 4) 5:1 LVII:DNA (w/w) (1:1 DOTAP:DOPE liposomes without QDs)

Lane 5) 0.75:1 LQDVII:DNA (w/w) (1:1 DOTAP:DOPE liposomes with CdSe/ZnS QDs)

Lane 6) 1.85:1 LQDVII:DNA

Lane 7) 3.71:1 LQDVII:DNA

Lane 8) 5.56:1 LQDVII:DNA

Lane 9) 7.41:1 LQDVII:DNA

Next, preparations of L-QDs incorporating cholesterol and cationic cholesterol derivative DC-Chol were tested to investigate their effect on transfection efficiency. Four compositions were tested:

L-QD Compositions (%molar ratio)

LQDA: 40% DOTAP, 30%DOPE, 15% Cholesterol, 15%DC-Cholesterol

LQDB: 40%DOTAP, 30%DOPE, 30%Cholesterol

LQDC: 40%DOTAP, 30%DOPE, 30%DC-Cholesterol

LQDVII: 50%DOTAP, 50%DOPE

Expression was observed by Western blot on cell lysates using dsRed Polyclonal

Primary antibody for detection. In all cases, those L-QDs that contained cholesterol and cholesterol derivatives performed better than those that did not (**Figure 3.17-3.20**). Furthermore, those formulations that contained at least 15% DC-Cholesterol (LQDA and LQDC) performed approximately two fold higher than those that did not. LQDA appears to perform the best out of all formulations as it exhibits fast turn-on and sustained expression throughout the study. LQDC also performs very well, showing excellent expression in later time points but appears to take longer to turn on effectively. LQDB also shows improved expression in later time points but in all cases does not approach either LQDA or LQDC. This illustrates the profound effect that cholesterol and cationic cholesterol-derivative DC-Cholesterol have on transfection efficiency of L-QDs in CHO cells.

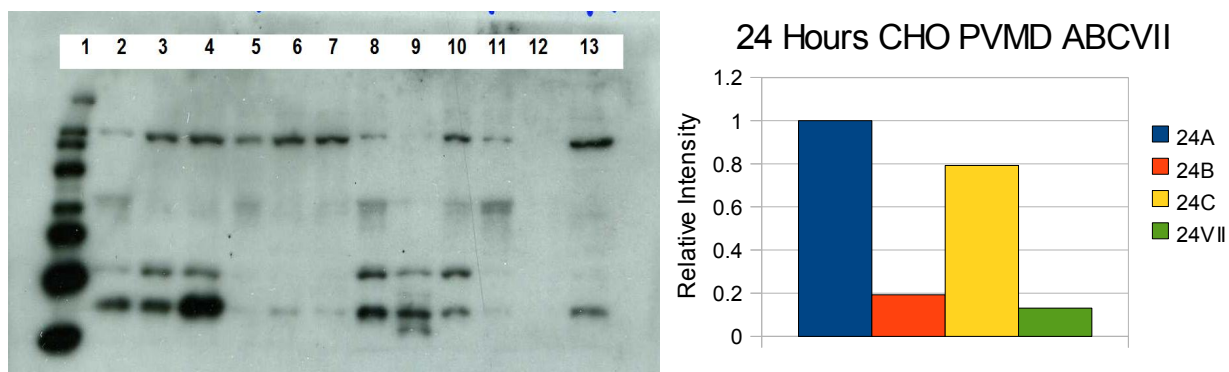


Figure 3.17: Expression of PV-mCherry in CHO at 24 hours post transfection using LQDA, LQDB, LQDC and LQDVII. (*Left*) Western blot of CHO cell lysates at 24 hours post transfection. **Lanes 1)** Magic Mark Size Marker, **2 – 4)** LQDA, **5 – 7)** LQDB, **8 – 10)** LQDC, **11 – 13)** LQDVII. (*Right*) Graph of integration of Western Blot Intensities relative to total protein concentration.

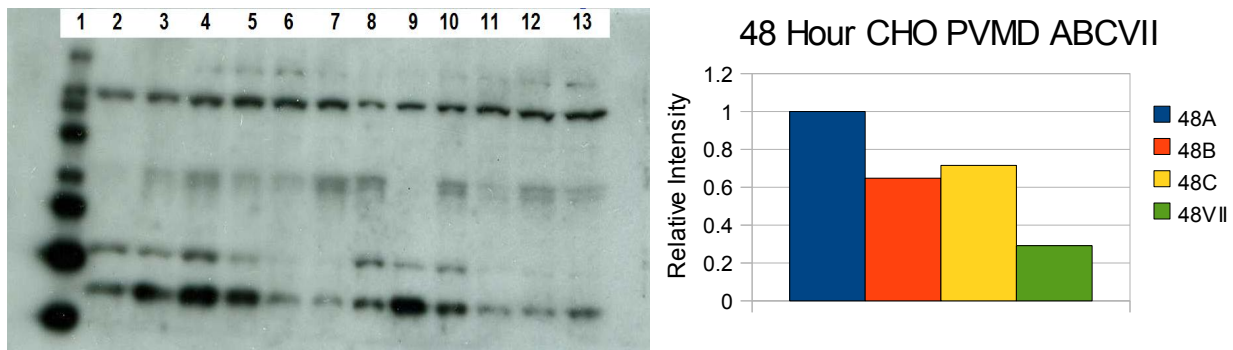


Figure 3.18: Expression of PV-mCherry in CHO at 48 hours post transfection using LQDA, LQDB, LQDC and LQDVII. (*Left*) Western blot of CHO cell lysates at 48 hours post transfection. **Lanes 1)** Magic Mark Size Marker, **2 – 4)** LQDA, **5 – 7)** LQDB, **8 – 10)** LQDC, **11 – 13)** LQDVII. (*Right*) Graph of integration of Western Blot Intensities relative to total protein concentration.

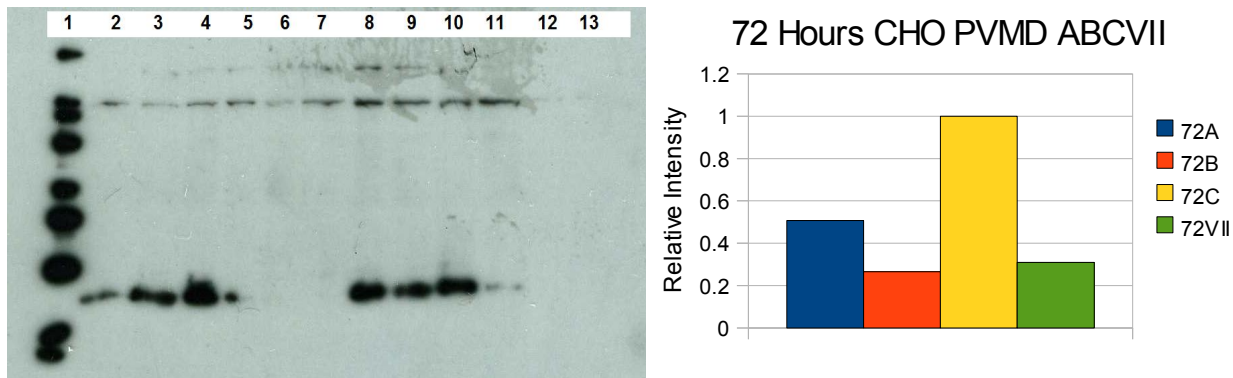


Figure 3.19: Expression of PV-mCherry in CHO at 72 hours post transfection using LQDA, LQDB, LQDC and LQDVII. (*Left*) Western blot of CHO cell lysates at 72 hours post transfection. **Lanes 1)** Magic Mark Size Marker, **2 – 4)** LQDA, **5 – 7)** LQDB, **8 – 10)** LQDC, **11 – 13)** LQDVII. (*Right*) Graph of integration of Western Blot Intensities relative to total protein concentration.

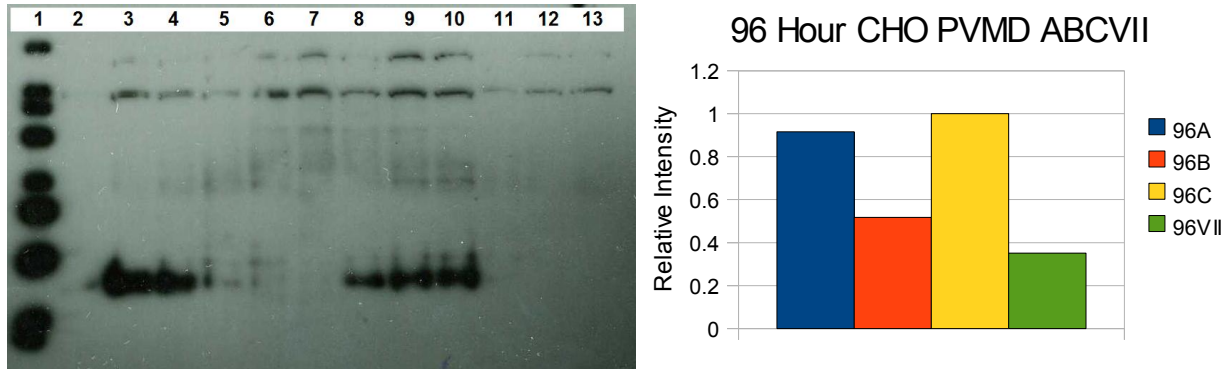


Figure 3.20: Expression of PV-mCherry in CHO at 96 hours post transfection using LQDA, LQDB, LQDC and LQDVII. (*Left*) Western blot of CHO cell lysates at 96 hours post transfection. **Lanes 1)** Magic Mark Size Marker, **2 – 4)** LQDA, **5 – 7)** LQDB, **8 – 10)** LQDC, **11 – 13)** LQDVII. (*Right*) Graph of integration of Western Blot Intensities relative to total protein concentration.

Now that a formulation of lipids has been established that provides robust and consistent expression (LQDA), it was of interest to investigate how well this formulation performed when compared to commercial reagent Optifect in CHO cells. The cell lysates of LQDA at 24, 48, 72 and 96hrs were run on a western blot and compared to the cell lysate of CHO cells transfected with Optifect at 48hrs post transfection (**Figure 3.21**). What was

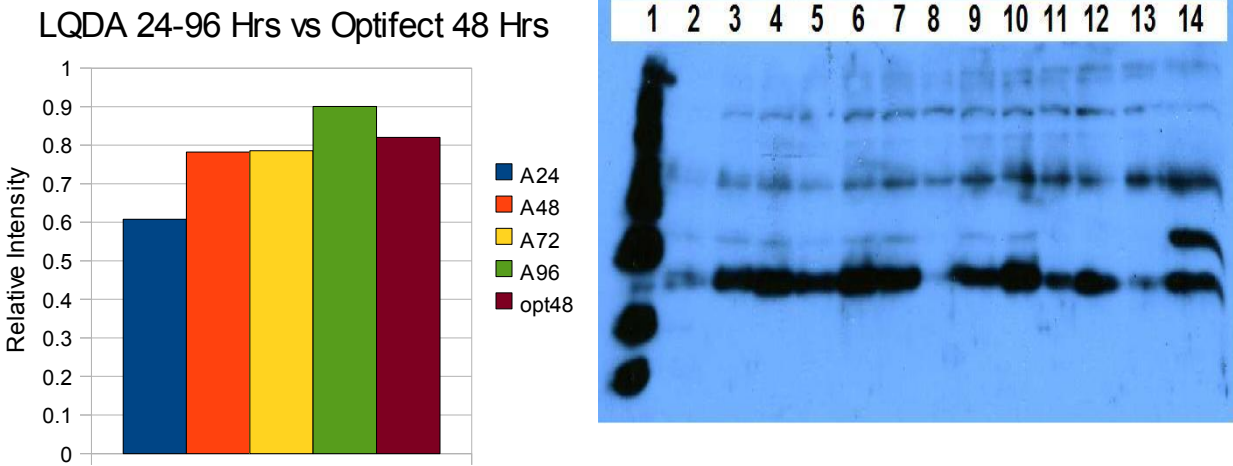


Figure 3.21: Expression of PV-mCherry delivered by LQDA at 24, 48, 72 and 96hr time points compared to expression of PV-mCherry delivered by Optifect at 48hrs. (Left) Graph of integration of Western Blot intensities relative to total protein concentration. (Right) Western Blot of PV-mCherry delivered by LQDA and Optifect, detected by dsRed Polyclonal primary antibody. **Lanes 1)** Magic Mark Size Marker **2 – 4)** LQDA 24 hrs **5 – 7)** LQDA 48 hrs **8 – 10)** LQDA 72 hrs **11 – 13)** LQDA 96 hrs **14)** Optifect 48 hrs

observed was that at 48hrs LQDA performs nearly as well as the commercial reagent Optifect, with expression continuing to increase throughout the 96 hr time course.

Therefore, it is reasonable to conclude that not only can L-QDs be used for the transfection of DNA into mammalian cells but that with the correct formulation of lipids, these L-QDs can perform at levels comparable to those of commercial origin, showing quick, robust and sustained expression over at least a 96 hour time course.

CHAPTER 4: CONCLUSIONS AND FUTURE DIRECTION OF RESEARCH

4.1 - Conclusions

Parvalbumin Major Isoform I was successfully cloned onto the N-terminus of the mCherry plasmid. The internal Kozak sequence of the fusion peptide was successfully removed by mutation. This gene was again successfully mutated to remove Hind III restriction enzyme cut site and then sub-cloned into α -MyHC promoter construct. Sequencing results show a perfect alignment and cloning was performed exactly as planned.

The expression of PV-mCherry (in CMV promoter plasmid) was observed by Western Blot, Fluorescence Microscopy and Flow Cytometry. As expected, no expression was observed in CHO cells for those transfected with α -MyHC PV-mCherry. Expression was observed for both delivery by commercial reagents and L-QDs.

Cationic Liposomes containing Quantum Dots are stable, small, unilamellar structures with QDs associated with the alkyl region of their bilayer. They exhibit cationic surface charge and readily associate with DNA. They are taken up by the cell and remain fluorescent for several days after uptake. The ability to deliver DNA appears to be highly affected by the presence of cholesterol and its derivatives with the combination of both yielding the best results. Due to the relatively high levels of expression observed for L-QDs relative to commercial reagents, it is reasonable to say that L-QDs are a suitable delivery method of plasmid DNA into mammalian cell cultures that contain built-in optical tracers.

4.2 Future Directions of Research

Because of the nature of the protein and promoter system developed, the obvious next move would be to attempt transfection of cardiomyocyte cultures with α -MyHC PV-mCherry using L-QDA formulation developed previously and investigating the effect of this expression on the rates of relaxation and contraction. If successful, then administering this system to the cardiac tissue of a live animal would be logical to test whether this delivery system can be used to safely treat a disease state *in vivo*. Also,

the integration of some PEGylated lipids into the L-QD formulations should be investigated. This should increase the circulation time of the L-QD – DNA complexes *in vivo*. Also, the co-delivery of a secondary effector could be performed. In this case, since the transfection of α -MyHC is sensitive to the presence of Thyroxine, it is reasonable to envision the encapsulation of Thyroxine into cationic liposomes, thus delivering a gene with cell-specificity along with a naturally occurring secondary effector that will up-regulate the transfection of the gene delivered. This could be done systemically, but hyperthyroidism has several negative effects which would be side-stepped by this approach.

The incorporation of QDs into cationic liposomes offers us the ability to label tumors and other tissue types as discussed elsewhere. It also gives us the ability to inexpensively deliver DNA and determine optically where our gene therapy products are localized in the body in the absence of fluorescent proteins or lipids, which are expensive and susceptible to chemical degradation and photobleaching. Due to the success of this system, it is also easy to envision the incorporation of magnetic materials such as Fe_3O_4 into cationic lipids. This would not only make it possible to follow the localization of gene therapy products in the body by MRI imaging but also begs the question as to whether the use of magnetic fields could be employed to target gene therapeutics to specific areas of the body. If so, then a mixture of magnetic and fluorescent materials can be employed to achieve a number of effects.

Another aspect of gene therapy which I feel has been largely overlooked is the use of mRNA for gene therapy. Although less stable and shorter-lived than its DNA counterpart, mRNA provides short, robust transfection events that are most likely much more suitable than DNA for the transfection of non-dividing cells since they do not require access to the nucleus. Also, with the use of mRNA, there is zero chance of mutation, insertion, etc and will be degraded quickly. Coupling mRNA and DNA delivery into a single vehicle could be employed to perform a number of feats, providing expression of a number of proteins. Time profiles of expression could be augmented by mixing ratios of mRNA:DNA with mRNA creating fast turn-on and DNA creating a more sustained expression pattern.

REFERENCES

- Al-Jamal, WT., et al, *Lipid-quantum dot bilayer vesicles enhance tumor cell uptake and retention in vitro and in vivo*, ACS Nano., 2008, 2: 408-418
- Bessis, N. et al, *Immune responses to gene therapy vectors: influence on vector function and effector mechanisms*, Gene Therapy, 2004, **11**: S10-7
- Bulte, J., et al., *Iron Oxide MR Contrast Agents for Molecular and Cellular Imaging*, NMR Biomed., 2004, **17**: 484-499
- Choi, H. S. et al, *Renal clearance of quantum dots*, Nat Biotechnol., 2007, **25(10)**: 1165-1170
- Coutu, P. et al, *Optimal Range for Parvalbumin as Relaxing Agent in Adult Cardiac Myocytes: Gene Transfer and Mathematical Modeling*. Biophysical Journal, 2002, **82**: p. 2565-2579
- Dabbousi, BO., et al, *(CdSe)ZnS Core-Shell Quantum Dots: Synthesis and Characterization of a Size Series of Highly Luminescent Nanocrystallites*, J. Phys. Chem. B, 1997, **101**: 9463-9475
- Felgner, P., et al, *Lipofection: A highly efficient, lipid-mediated DNA-transfection procedure*, Proc. Nat. Acad. Sci., 1987, **84**: 7413-7417
- Ghosh, P., et al., *Efficient Gene Delivery Vectors by Tuning the Surface Charge Density of Amino Acid-Functionalized Gold Nanoparticles*, ACS Nano, **2008**, 2 (11): 2213-2218
- Gulick, J. et al, *Isolation and Characterization of the Mouse Cardiac Myosin Heavy Chain Genes*, J. Bio. Chem., 1991, **266**: p. 9180-9185
- Hauck, TS., et al., *In Vivo Quantum-Dot Toxicity Assessment*, Small, 2010, **6**: 138-144
- Igor, L., et al., *Quantum Dot Bioconjugates for Imaging, Labelling and Sensing*, Nature Materials, 2005, **4**: 435-446
- Kalyuzhny, G., et al., *Ligand Effects on Optical Properties of CdSe Nanocrystals*, J. Phys. Chem. B, 2005, **109**: 7012 – 7021
- Li, D. et al, *Glutathione-Mediated Release of Functional Plasmid DNA from Positively Charged Quantum Dots*, Biomaterials, 2008, **29**: p. 2776-2782
- Lloyd-Jones, D., et al., *Heart Disease and Stroke Statistics 2010 Update A Report from the American Heart Association*, Circulation, 2009, published online doi: **10.1161/CIRCULATIONAHA.109.192667**

- Lozell, B., *Significance of Diastolic Dysfunction of the Heart*. Annu. Rev. Med., 1991, **42**: p. 411-436
- Lv, H., et al., *Toxicity of cationic lipids and cationic polymers in gene delivery*, Journal of Controlled Release, 2006, **114**: 100-109
- Mitchell, GP., et al., *Programmed Assembly of DNA Functionalized Quantum Dots*, J. Am. Chem. Soc., 1999, **121**: 8122-8123
- Oishi, M., et al., *Smart PEGylated Gold Nanoparticles for the Cytoplasmic Delivery of siRNA to Induce Enhanced Gene Silencing*, Chem. Lett., 2006, **35**: no 9
- Rindt, H. et al, *An in vivo Analysis of Transcriptional Elements in the Mouse α -Myosin Heavy Chain Gene Promoter*, Transgenic Research, 1995, **4**: p. 397-405
- Robbins, J., *Altering Cardiac Function via Transgenesis; A Nuts and Bolts Approach*, TCM, 1997, **7**: p. 185-191
- Robert, W., et al., *Cationic Liposome-Mediated RNA Transfection*, Proc. Natl. Acad. Sci., 1989, **86**: 6077-6081
- Sakurai, F., et al, *Effect of DNA/liposome mixing ratio on the physiochemical characteristics, cellular uptake and intracellular trafficking of plasmid DNA/ cationic liposome complexes and subsequent gene expression*, Journal of Controlled Release, 2000, **66**: 255-269
- Tripathy, S.K. et al, *Immune Responses to Transgene-Encoded Proteins Limit the Stability of Gene Expression after Injection of Replicative-Defective Adenovirus Vectors*, Nat. Med. 1996, **2(5)**: p. 545-550
- Wahr, P., et al, *Parvalbumin Gene Transfer Corrects Diastolic Dysfunction in Diseased Cardiac Myocytes*. PNAS, 1999, **96**: p. 11982-11985
- Washington, AL., et al, *Microwave Synthesis of CdSe and CdTe nanocrystals in nonabsorbing alkanes*, J Am Chem Soc., 2008, **130**: 8916-8922
- Zidovska, A., et al, *The Role of Cholesterol and Structurally Related Molecules in Enhancing Transfection of Cationic Liposome – DNA Complexes*, J. Phys. Chem. B., 2009, **113**: 5208 – 5216

BIOGRAPHICAL SKETCH

B. August 20th, 1983 in Miami, Florida.

High School 1998 - 2001

Sweet Home Senior High School, Class of 2001.

B.S. 2001 - 2006

Florida State University, Majors in Chemistry and Biochemistry, Minors in Mathematics, Physics and Biology

M.S. 2007 – 2010

Florida State University, Molecular Biophysics Program, later transferring to Department of Chemistry and Biochemistry. Program in Biochemistry.